



Review

# Machine Learning Styles for Diabetic Retinopathy Detection: A Review and Bibliometric Analysis

Shyamala Subramanian <sup>1,2,\*</sup>, Sashikala Mishra <sup>1</sup>, Shruti Patil <sup>3</sup> , Kailash Shaw <sup>1,\*</sup> and Ebrahim Aghajari <sup>4</sup>

<sup>1</sup> Symbiosis Institute of Technology, Pune (SIT), Symbiosis International (Deemed) University (SIU), Pune 412115, India

<sup>2</sup> Department of Electronics and Telecommunication, SIES Graduate School of Technology, Navi Mumbai 400706, India

<sup>3</sup> Symbiosis Centre for Applied Artificial Intelligence (SCAAI), Symbiosis Institute of Technology, Symbiosis International (Deemed) University (SIU), Pune 412115, India

<sup>4</sup> Department of Electrical Engineering, Ahvaz Branch, Islamic Azad University, Ahvaz 61349-37333, Iran

\* Correspondence: shyamalamathi123@gmail.com (S.S.); kailash.shaw@gmail.com (K.S.)

**Abstract:** Diabetic retinopathy (DR) is a medical condition caused by diabetes. The development of retinopathy significantly depends on how long a person has had diabetes. Initially, there may be no symptoms or just a slight vision problem due to impairment of the retinal blood vessels. Later, it may lead to blindness. Recognizing the early clinical signs of DR is very important for intervening in and effectively treating DR. Thus, regular eye check-ups are necessary to direct the person to a doctor for a comprehensive ocular examination and treatment as soon as possible to avoid permanent vision loss. Nevertheless, due to limited resources, it is not feasible for screening. As a result, emerging technologies, such as artificial intelligence, for the automatic detection and classification of DR are alternative screening methodologies and thereby make the system cost-effective. People have been working on artificial-intelligence-based technologies to detect and analyze DR in recent years. This study aimed to investigate different machine learning styles that are chosen for diagnosing retinopathy. Thus, a bibliometric analysis was systematically done to discover different machine learning styles for detecting diabetic retinopathy. The data were exported from popular databases, namely, Web of Science (WoS) and Scopus. These data were analyzed using Biblioshiny and VOSviewer in terms of publications, top countries, sources, subject area, top authors, trend topics, co-occurrences, thematic evolution, factorial map, citation analysis, etc., which form the base for researchers to identify the research gaps in diabetic retinopathy detection and classification.

**Keywords:** machine learning; deep learning; diabetic retinopathy; fundus images



**Citation:** Subramanian, S.; Mishra, S.; Patil, S.; Shaw, K.; Aghajari, E. Machine Learning Styles for Diabetic Retinopathy Detection: A Review and Bibliometric Analysis. *Big Data Cogn. Comput.* **2022**, *6*, 154. <https://doi.org/10.3390/bdcc6040154>

Academic Editor: Moulay A. Akhloufi

Received: 15 October 2022

Accepted: 25 November 2022

Published: 12 December 2022

**Publisher's Note:** MDPI stays neutral with regard to jurisdictional claims in published maps and institutional affiliations.



**Copyright:** © 2022 by the authors. Licensee MDPI, Basel, Switzerland. This article is an open access article distributed under the terms and conditions of the Creative Commons Attribution (CC BY) license (<https://creativecommons.org/licenses/by/4.0/>).

## 1. Introduction

Nowadays, many people are suffering from diabetic retinopathy (DR). It is one of the most typical reasons among adults aged 20–74 years for blind registration in the world [1]. Retinopathy development depends on how long a person has had diabetes. The prevalence of diabetes in India alone was 11.8%, with 10.7%, 13.1%, 13.2%, and 9.7% in the 50–59 years age group, 60–69 years age group, 70–79 years age group, and ≥80 years age group, respectively, from 2015 to 2019 [2] (Figure 1). In the 70–79 years age group, the prevalence of diabetes was the highest.

This prolonged diabetes leads to diabetic retinopathy. DR affects the vision of 463 million people worldwide and is responsible for 22.27% of global blindness (2019) [1]. In India, 16.9% [2] (Figures 2 and 3), i.e., around 72.96 million cases in the population, are suffering from DR, as per a survey done from 2015 to 2019. *The Times of India* article dated 14th Nov 2021 reported 77 million DR cases in India [3]. The cases increased mainly due to type 2 diabetes.

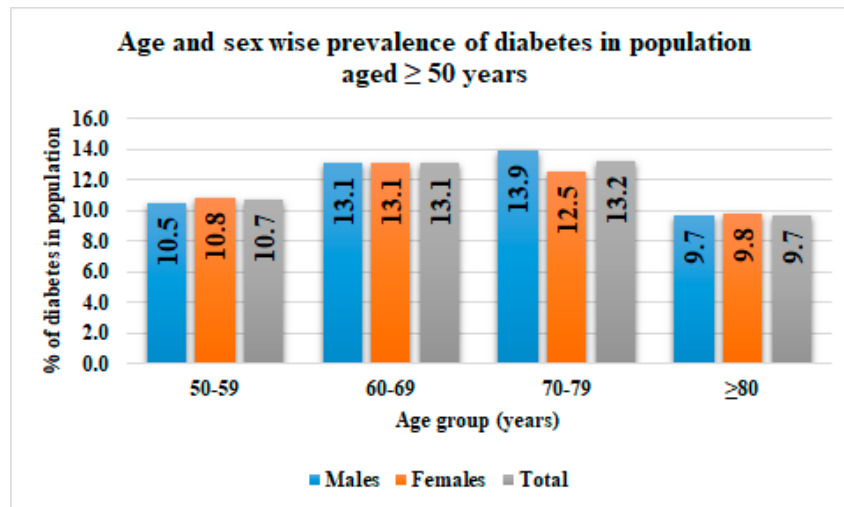


Figure 1. Age-wise and sex-wise prevalence of diabetes in the population aged  $\geq 50$  years.

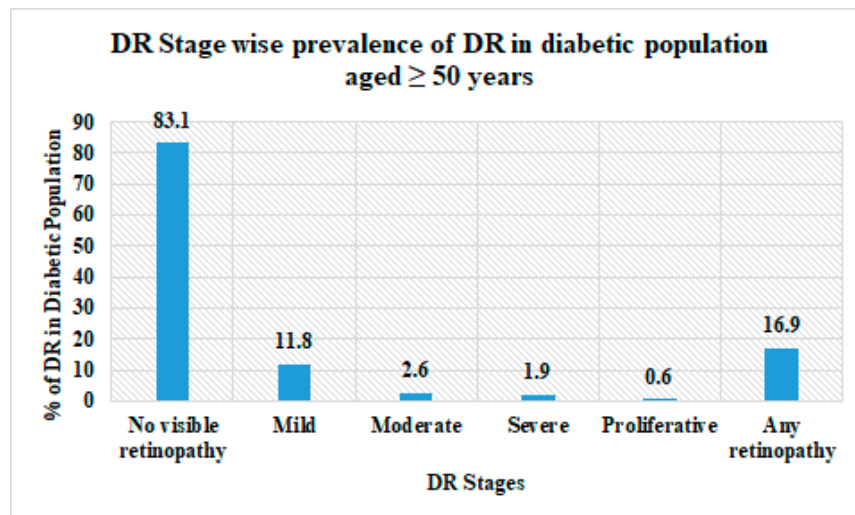


Figure 2. DR stage-wise prevalence of DR in the diabetic population.

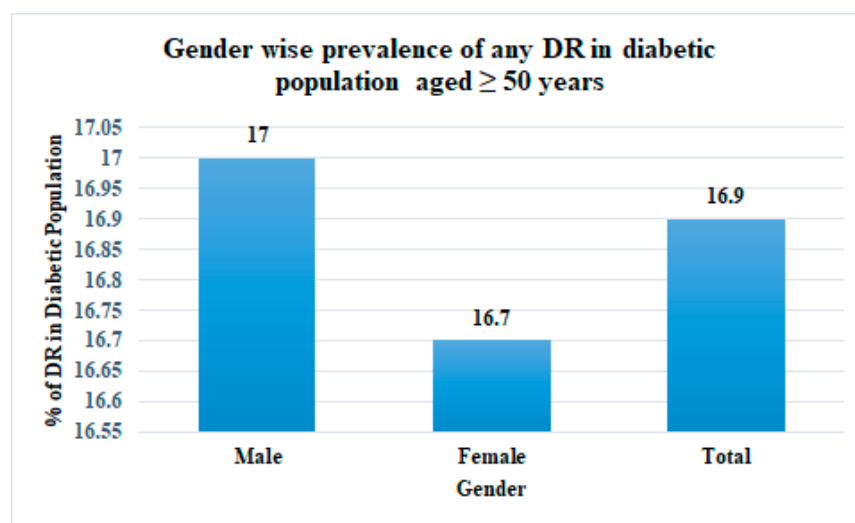
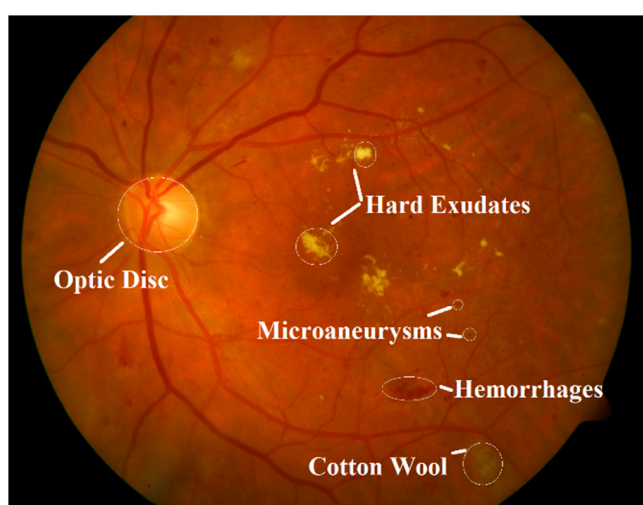


Figure 3. Gender-wise prevalence of any DR in the diabetic population aged  $\geq 50$  years.

The traditional screening of fundus images for diagnosing DR lesions takes time, thereby delaying therapy and reducing the chance of success. Therefore, the screening strategies must be changed to save the time of both doctors and patients by using a computer-aided diagnosis. Thus, new technologies, such as machine learning, come into play for detecting and classifying DR. The quality, affordability, and accessibility of DR screening in the diabetic population are all crucial parameters in preventing blindness. New technology will ease this issue in terms of cost.

In DR patients, lesions [4] such as microaneurysms, hemorrhages, exudates, and neovascularization (Figure 4) may develop. These lesions need to be detected early for proper intervention. Microaneurysms are small swellings that form at the internal wall of a blood vessel, which may burst and leak blood into nearby tissues, whereas hemorrhages are ruptures of capillaries. Exudates can be hard exudates or soft exudates. Hard exudates are yellowish lipids that leak from an abnormal blood vessel, and soft exudates are whitish-grey, also called cotton wool.



**Figure 4.** Diabetic retinopathy retinal image showing lesions.

Diabetic retinopathy is divided into two types: non-proliferative and proliferative. Non-proliferative DR is divided into three stages: mild, moderate, and severe [5]. Only microaneurysms are present in mild non-proliferative DR, while exudates characterize moderate and severe stages, along with microaneurysms. However, microaneurysms may be present in later stages. During non-proliferative DR, the patient barely experiences any peculiar symptoms. However, their eyesight gradually becomes impaired as the disease progresses to the proliferative stage. It may lead to neovascularization; thus, the patient may lose vision completely. Therefore, intervention at a later stage is less helpful, and thus, diagnosing DR early is necessary [6].

Artificial intelligence and machine learning have been widely employed in healthcare, especially for disease diagnosis. Thus, a computer-based diagnosis is required to accurately identify diabetic retinopathy symptoms for early intervention. Many studies were carried out using machine learning techniques to process medical images automatically and diagnose diseases. We categorized them based on their learning styles. This study will be helpful for researchers to acquire insights into the application of AI-ML in the research of diabetic retinopathy from the year 2000 to 2021. We used bibliometric analysis to analyze papers related to machine-learning-based diabetic retinopathy. The data was collected from the Scopus and WoS databases. An intensive quantitative study was done using VOSViewer, Gephi, Rstudio, and Biblioshiny regarding the top author's production over time, trend topic, keywords analysis, thematic evolution, etc. Furthermore, the fundamental analysis, such as yearly publication, number of citations per year, top countries, etc., was done using Excel.

The rest of the paper is designed as follows: Section 2 outlines the search strategy utilized in data collection from Scopus and WoS databases. The analysis results of the collected data are given in Section 3 in various ways, such as documents published per year, the number of citations per year, source analysis, top countries, and top authors involved in research, and keyword analysis. Section 4 expounds on the qualitative study based on different machine learning styles used in the literature. Section 5 summarizes the paper and exhibits a few issues. Finally, Section 6 concludes the article.

## 2. Research Methodology

Quantitative and qualitative analyses are the two crucial strategies used for collecting and deciphering data in research. Both quantitative and qualitative analyses were carried out in this paper, which will help research scholars to refine their research area and identify the research gaps.

Bibliometric analysis thoroughly examines the research carried out in a particular area. It is the factual investigation of journals, articles, books, or other distributions. This particular analysis assessed the significance and impact of journals and articles published in detecting diabetic retinopathy and may offer assistance regarding treatment advancement, as well as helping with financing and grants.

This research aimed to look into various machine learning algorithms for diabetic retinopathy detection, and thus, identify the areas of opportunity to improve the performance of machine learning for detecting DR.

### Search Strategy

The data were collected from the most popularly known databases, i.e., Scopus and Web of Science (WoS). Figure 5 shows the search query [7] used in both databases for this study.

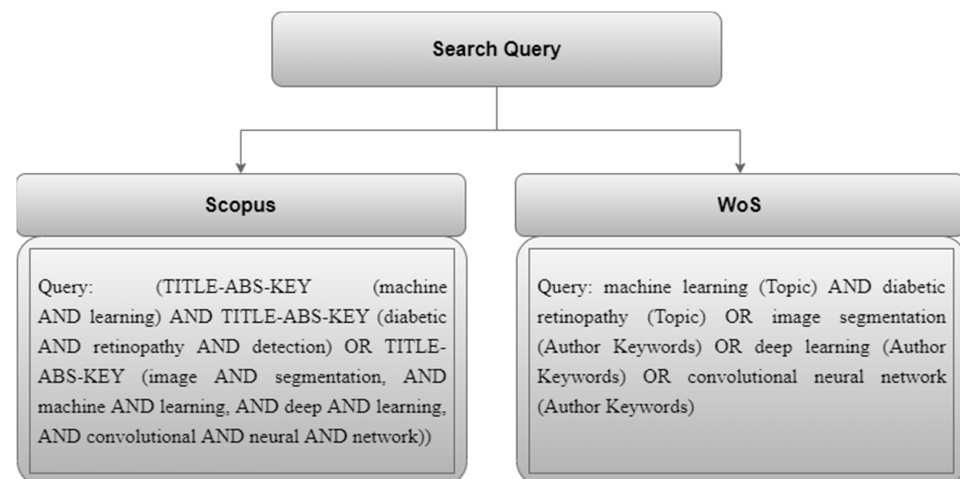


**Figure 5.** Search queries.

The search strategy [8] is shown in Figure 6, where a total of 472 documents from Scopus and 538 from WoS met the selection criteria for all different document types from 2000 to 2021. The documents were articles, conference papers, review articles, conference reviews, book chapters, letters, abstracts, meetings, early access, editorial materials, and data papers.

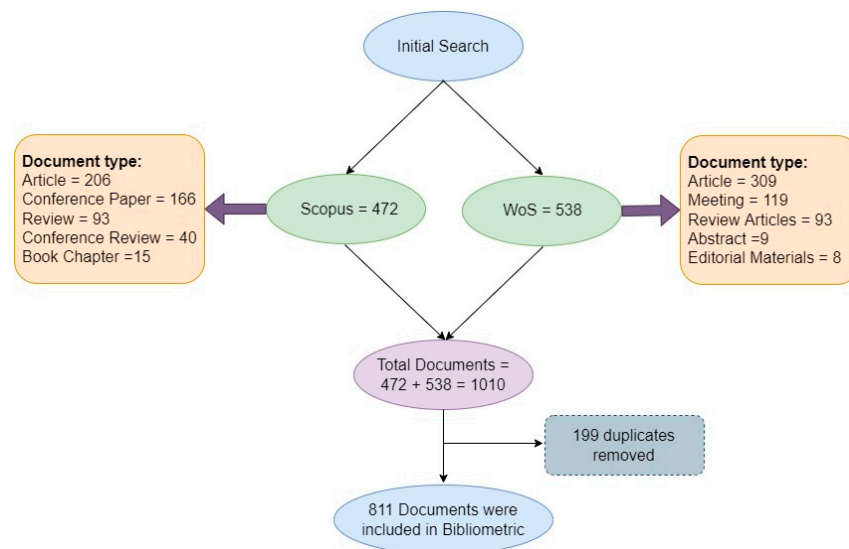


Figure 6. Search strategy.

### 3. Quantitative Analysis

The comma-separated values (CSV) file downloaded from Scopus contained all the articles with the author, ID, title, year, source title, volume, issue, page start, page end, page count, cited by, DOI, link, affiliations, author keywords, publisher, ISSN, ISBN, document type, source type, and PubMed ID information. The text file downloaded from WoS contained all the articles with the details of the publication type, authors, book authors, article title, patent number, source title, volume, issue, DOI, publication year, ISSN, ISBN, unique ID, and PubMed ID.

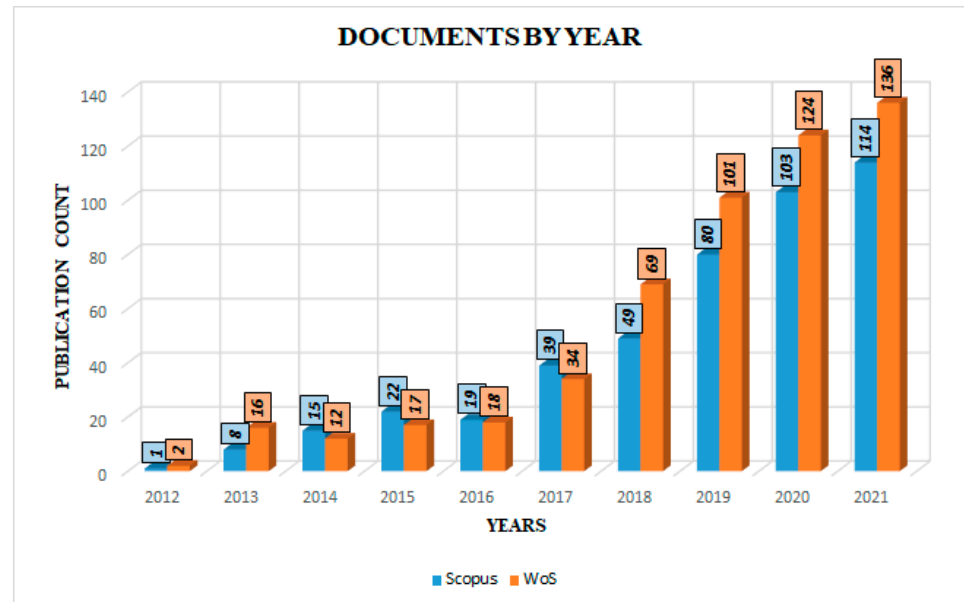
We thoroughly analyzed (Figure 7) this information using Excel, RStudio, Biblioshiny, and VOSviewer to quantify the amount of work done in detecting diabetic retinopathy using machine learning.



Figure 7. Quantitative analysis.

### 3.1. Publication Analysis

Figure 8 shows a bar graph of the number of documents published yearly in Scopus and WoS from 2012 onward. Researchers started working on diabetic retinopathy detection using machine learning in 2000. Initially, very few papers were published, and after 2013, we found a substantial increase in publications, with 114 (Scopus) and 136 (WoS) in 2021.



**Figure 8.** Year-wise number of documents published in Scopus and WoS.

### 3.2. Citation Analysis

The comparative analysis of citation received per year for the papers published in both databases are tabulated, as shown in Table 1, which indicated that around 1000 more citations were received for the documents published in WoS.

**Table 1.** Comparative yearly citation analysis.

Database/Year	<2017	2017	2018	2019	2020	2021	Total
SCOPUS Citations	4308	2270	1322	793	768	88	9549
Web of Science Citations	3822	1608	1955	1930	926	248	10,489

The detailed analysis is shown graphically in Figure 9. It was observed that several citations received were at the peak for the papers published in the year 2016. One of the documents received 2571 out of 2827 citations (Scopus) and 2386 out of 2531 citations (WoS) in 2016. The document titled “Development and validation of a deep learning algorithm for the detection of diabetic retinopathy in retinal fundus photographs” was published in *JAMA—Journal of the American Medical Association* by Gulshan V et al. [9] and was included in both the databases and referred to by many researchers.

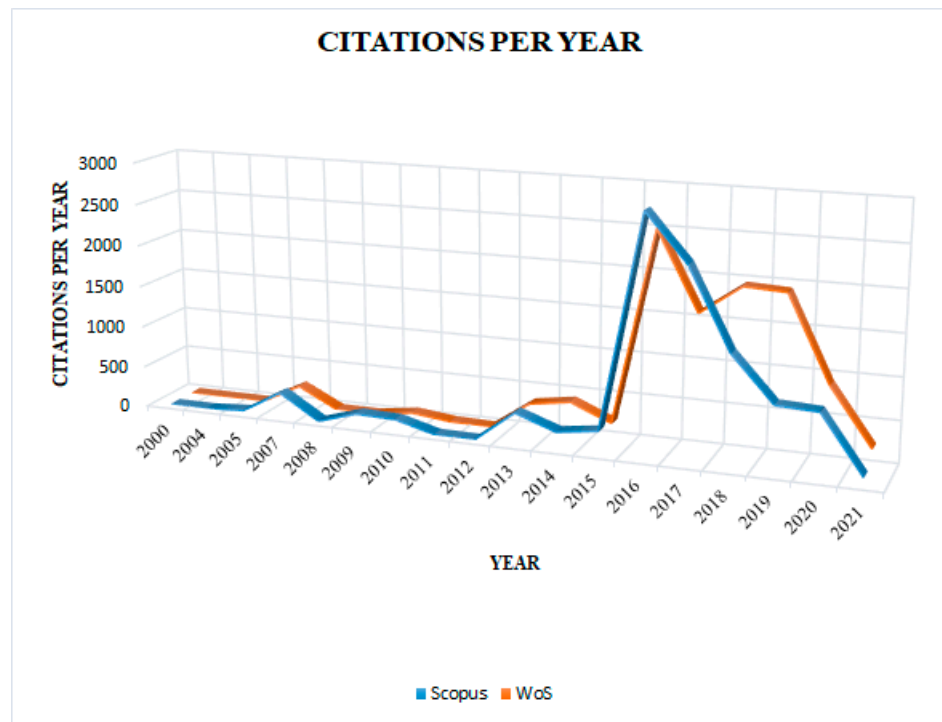


Figure 9. The number of citations per year.

### 3.3. Country Analysis

The analysis shows that 24 out of 57 countries published at least five documents with at least five citations. The following graph (Figure 10) shows the top 10 countries with at least five papers and at least five citations. From the analysis (Table 2), it is clear that the United States published fewer documents than India, but the average number of citations received was higher.

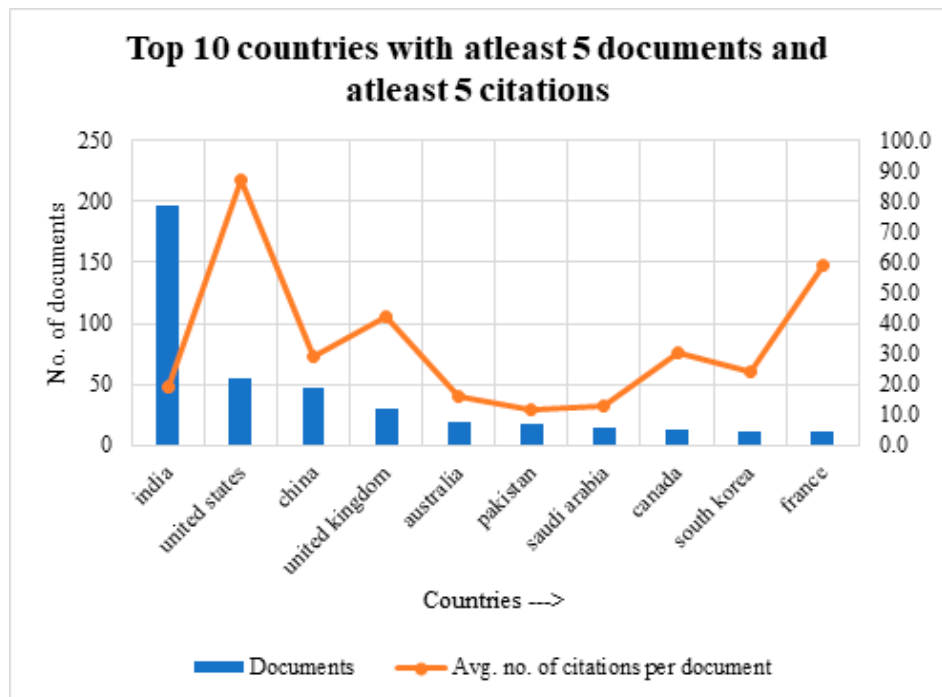


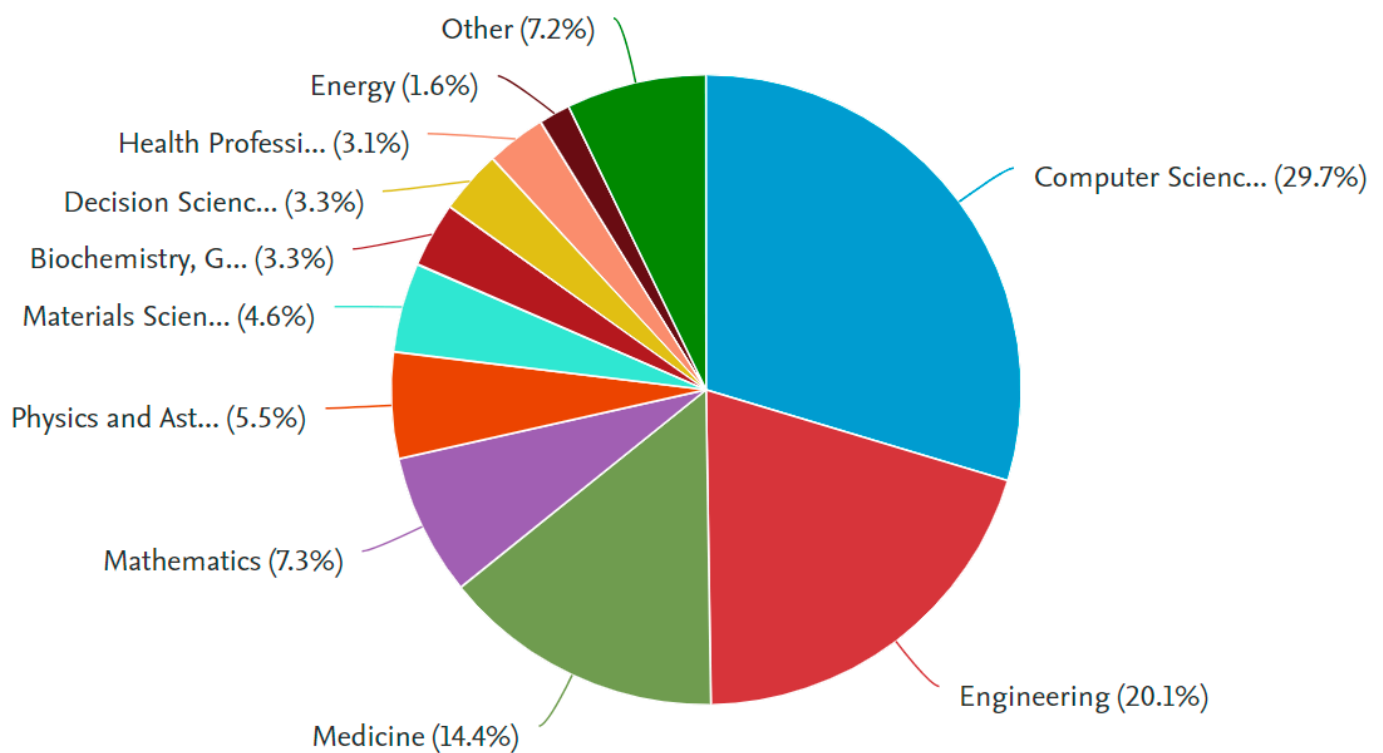
Figure 10. Number of documents published and citations received by the top 10 countries.

**Table 2.** List of top countries with the no. of documents and citations.

Country	No. of Documents	No. of Citations	Total Link Strength	Avg. No. of Citations per Document
India	197	3778	342	19.2
United States	55	4784	341	87
China	47	1382	196	29.4
United Kingdom	30	1271	145	42.4
Australia	20	324	81	16.2
Pakistan	18	211	78	11.7
Saudi Arabia	15	193	69	12.9
Canada	13	397	84	30.5
South Korea	12	287	74	23.9
France	11	649	83	59

### 3.4. Subject Area Analysis

The highest proportion of the work was done in the computer science field at 29.7% and in the engineering domain at 20.1% (Figure 11). Of course, people in the medical area were also working to find a solution for automated diagnosis.

**Figure 11.** Analysis of documents by subject area.

### 3.5. Sources Analysis

Out of 271 sources, the top 10 sources (Figure 12) were identified in this research field, which will cast some light and provide the right direction for future research.

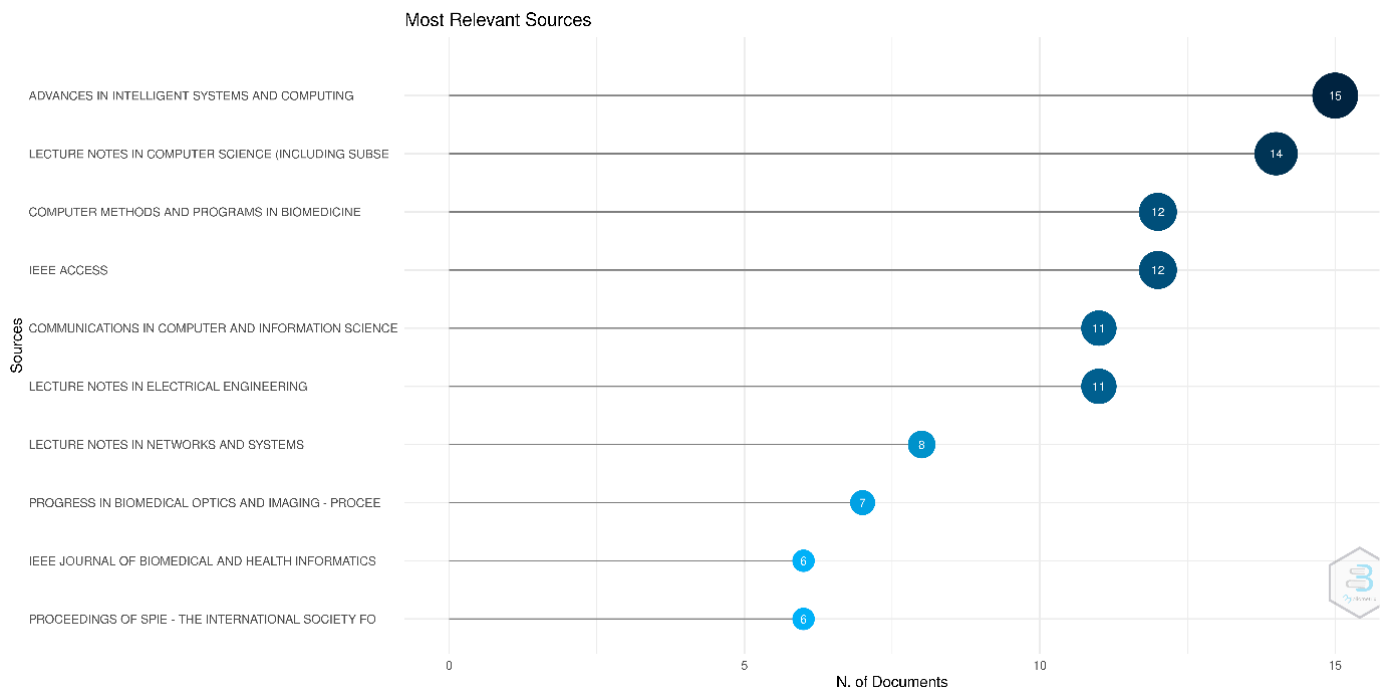


Figure 12. Top 10 most relevant sources.

### 3.6. Top Authors' Production over Time

The papers produced by the top 10 authors were analyzed over time (Figure 13). S. Banerjee [10] started working in this area in 2016 with one paper with total citations per year of 2.29. T. Peto [11] and M. Lamard [12] started their research around 2010, working till 2021 with five and seven articles, respectively. The top authors' production over time in terms of the no. of papers and total citations per year was plotted (Figure 13) and listed in tabular form (Table 3).

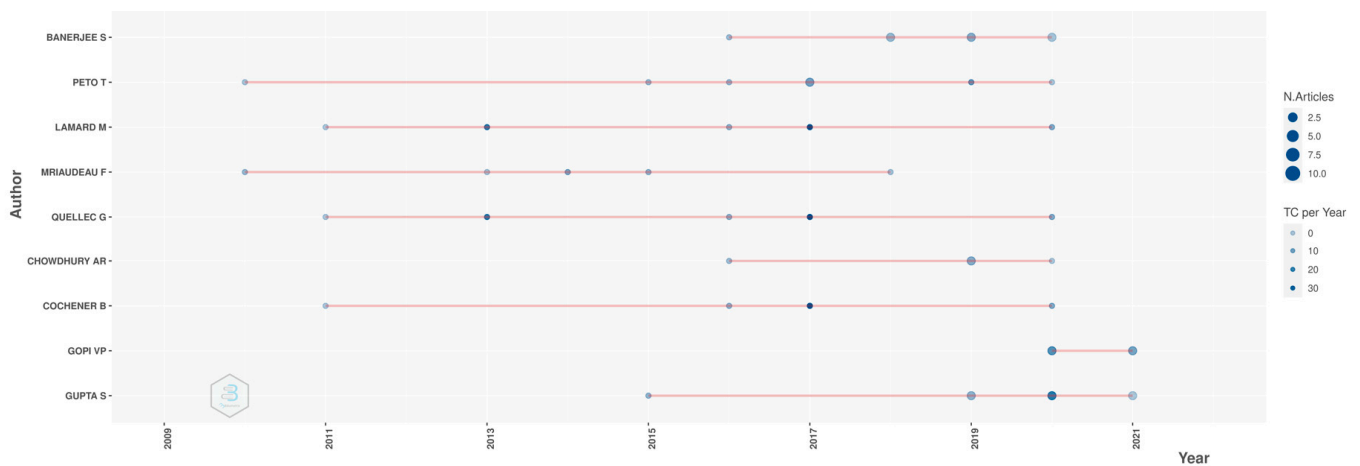


Figure 13. Top 10 authors' production over time.

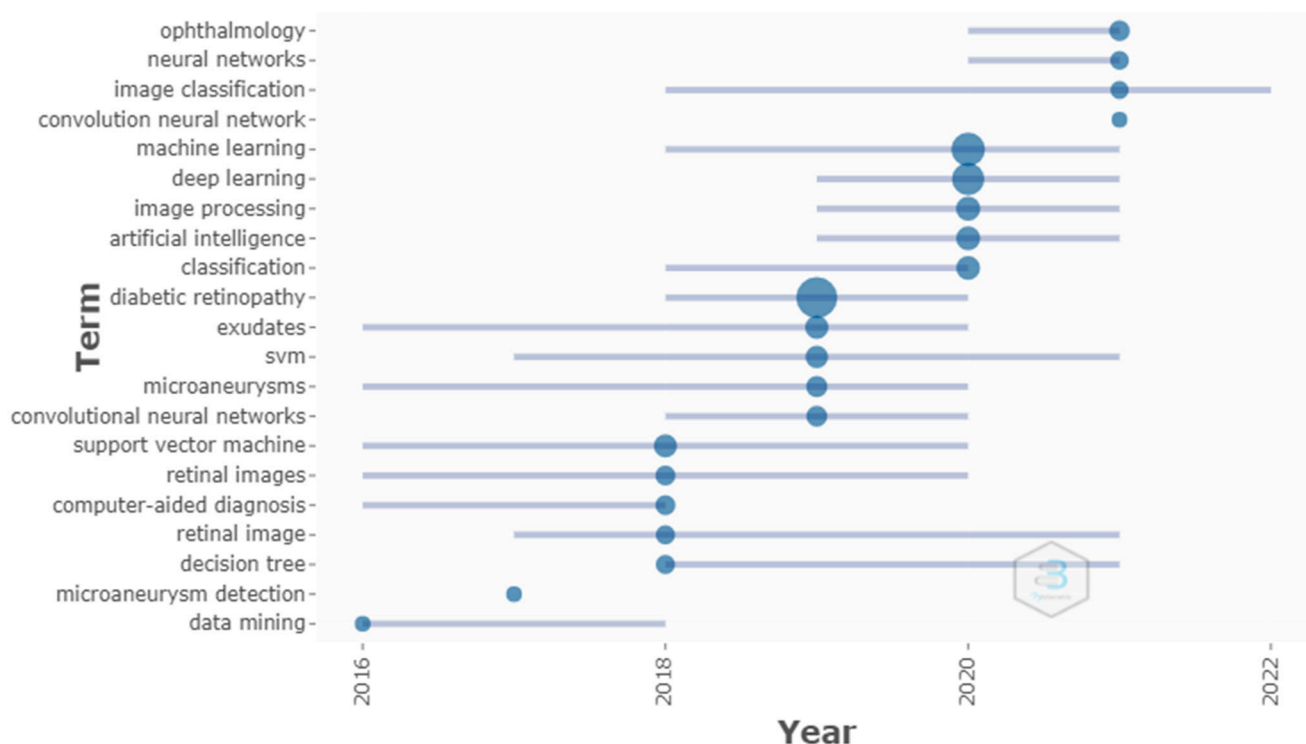
**Table 3.** No. of articles and total citations per year for the top authors.

AUTHOR	YEAR	2010	2011	2012	2013	2014	2015	2016	2017	2018	2019	2020	2021
BANERJEE S	No. of articles							1		2	2	2	
	Total citations per year (TCpY)							2.29		3	5.5	0.33	
PETO T	No. of articles	1					1	1	2		1	1	
	Total citations per year (TCpY)	1					3.25	3.43	8.83		10.3	0.33	
LAMARD M	No. of articles		1		1			1	1			1	
	Total citations per year (TCpY)		0.08		20.7			4.71	29.7			5.33	
MRIAUDEAU F	No. of articles	1			1	1	1			1			
	Total citations per year (TCpY)	3.54			1.2	8	4.63			1.2			
QUELLEC G	No. of articles		1		1			1	1			1	
	Total citations per year (TCpY)		0.08		20.7			4.71	29.7			5.33	
CHOWDHURY AR	No. of articles							1			2	1	
	Total citations per year (TCpY)							2.29			5.5	0	
COCHENER B	No. of articles		1					1	1			1	
	Total citations per year (TCpY)		0.08					4.71	29.7			5.33	
GOPI VP	No. of articles											2	2
	Total citations per year (TCpY)											10.3	5
GUPTA S	No. of articles						1				2	2	2
	Total citations per year (TCpY)						4.63				4	14.7	0

### 3.7. Trend Topic Analysis

We analyzed the authors' keywords over the period (2010 to 2021) and identified the trend of the keywords used. Terms such as exudates, microaneurysm, SVM, and computer-aided diagnosis appeared in 2016. These terms indicated that SVM classifiers were used to detect exudates and microaneurysms in most of the papers. Similarly, we found that decision trees were used in addition to SVM in 2018. More emphasis was given to the keyword diabetic retinopathy. Later, in the year 2020, machine learning and deep learning became the trend (Figure 14) to be used.

## Trend Topics



Term	Frequency	Term	Frequency	Term	Frequency
ophthalmology	13	artificial intelligence	28	support vector machine	23
neural networks	8	classification	27	retinal images	11
image classification	7	diabetic retinopathy	218	computer-aided diagnosis	11
convolution neural network	5	exudates	24	retinal image	9
machine learning	111	svm	20	decision tree	9
deep learning	96	microaneurysms	15	microaneurysm detection	5
image processing	29	convolutional neural networks	14	data mining	5

Figure 14. Trend topics over time.

### 3.8. Author Keyword Co-Occurrence Analysis

The analysis was carried out on keywords with at least ten occurrences (Figure 15). The authors defined 831 keywords, of which 32 met the threshold of 30 occurrences. The keywords deep learning occurred 95 times with 207 total link strengths, followed by image processing, artificial intelligence, convolutional neural network, etc., with fewer times. Of course, the search keywords will occur the highest number of times. Four clusters were formed, with 11 items in cluster 1, 9 in cluster 2, 7 in cluster 3, and 5 in cluster 4, which are indicated by red, green, blue, and yellow regions in the figure, respectively.

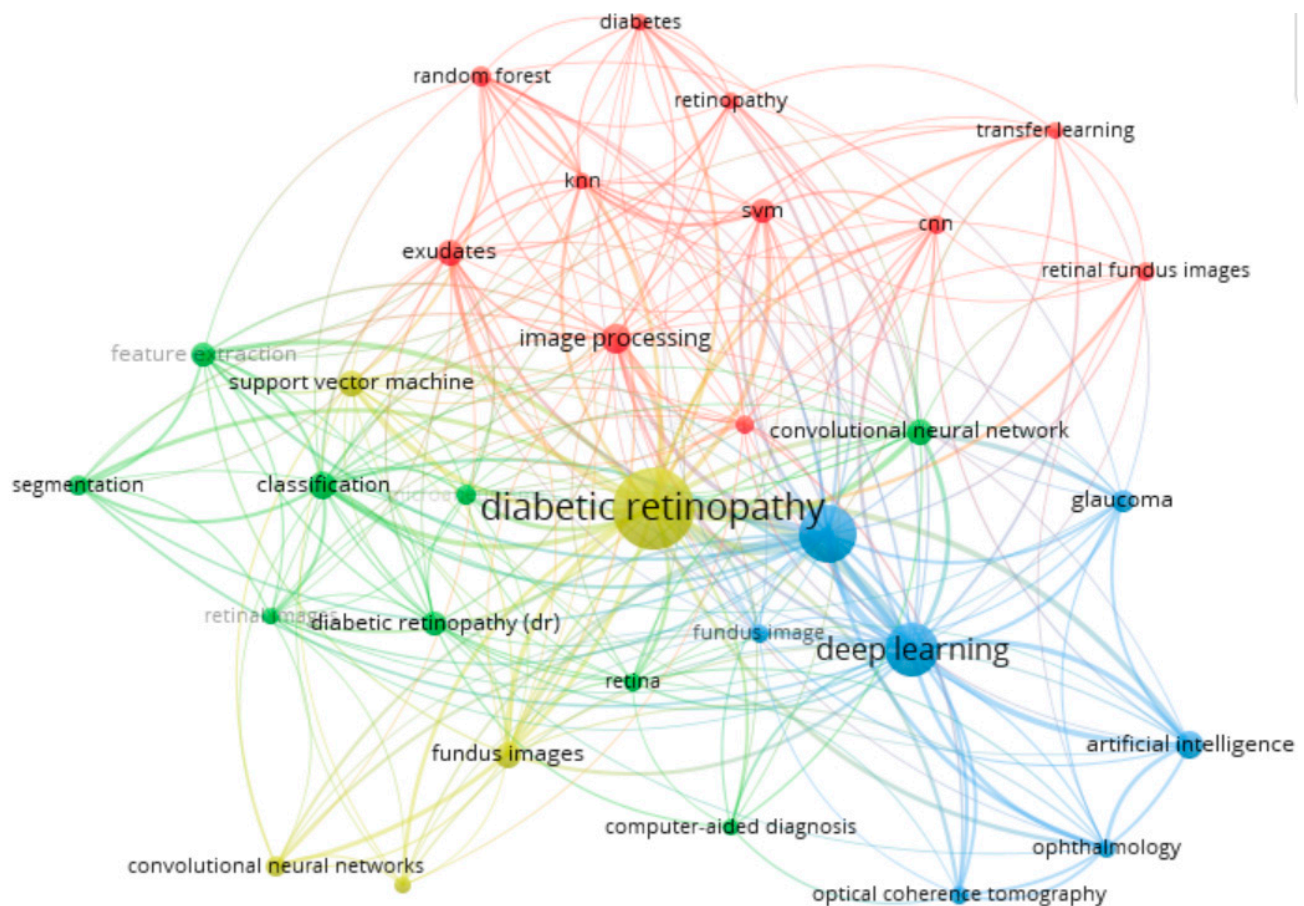


**Figure 15.** Author keyword co-occurrence analysis.

### 3.9. Conceptual Structure Map

The conceptual structure map was obtained from Biblioshiny using the multiple component analysis (MCA) method. This method is commonly used to analyze categorical data, which seeks to narrow down a vast number of variables into smaller sets of components that sum up the information in the data [13]. The conceptual structure is shown in Figure 16. It was found that exudate and microaneurysm lesions were detected by using SVM, random forest, kNN, and decision tree machine learning algorithms, which formed a single cluster. Author keywords such as ophthalmology, age-related macular degeneration, and optical coherence tomography were most frequently used, along with artificial intelligence, creating a second cluster. The maximum number of author keywords belonged to the third cluster, which included retinal landmarks (optic disc), lesions (hemorrhages, hard exudates), and fundus images. Moreover, most papers used the terms segmentation and machine learning techniques such as SVM, kNN, and advanced techniques such as deep learning, extreme learning machine, and transfer learning. The segmentation was generally used to locate retinal landmarks, lesions, etc., and machine learning techniques for classification.

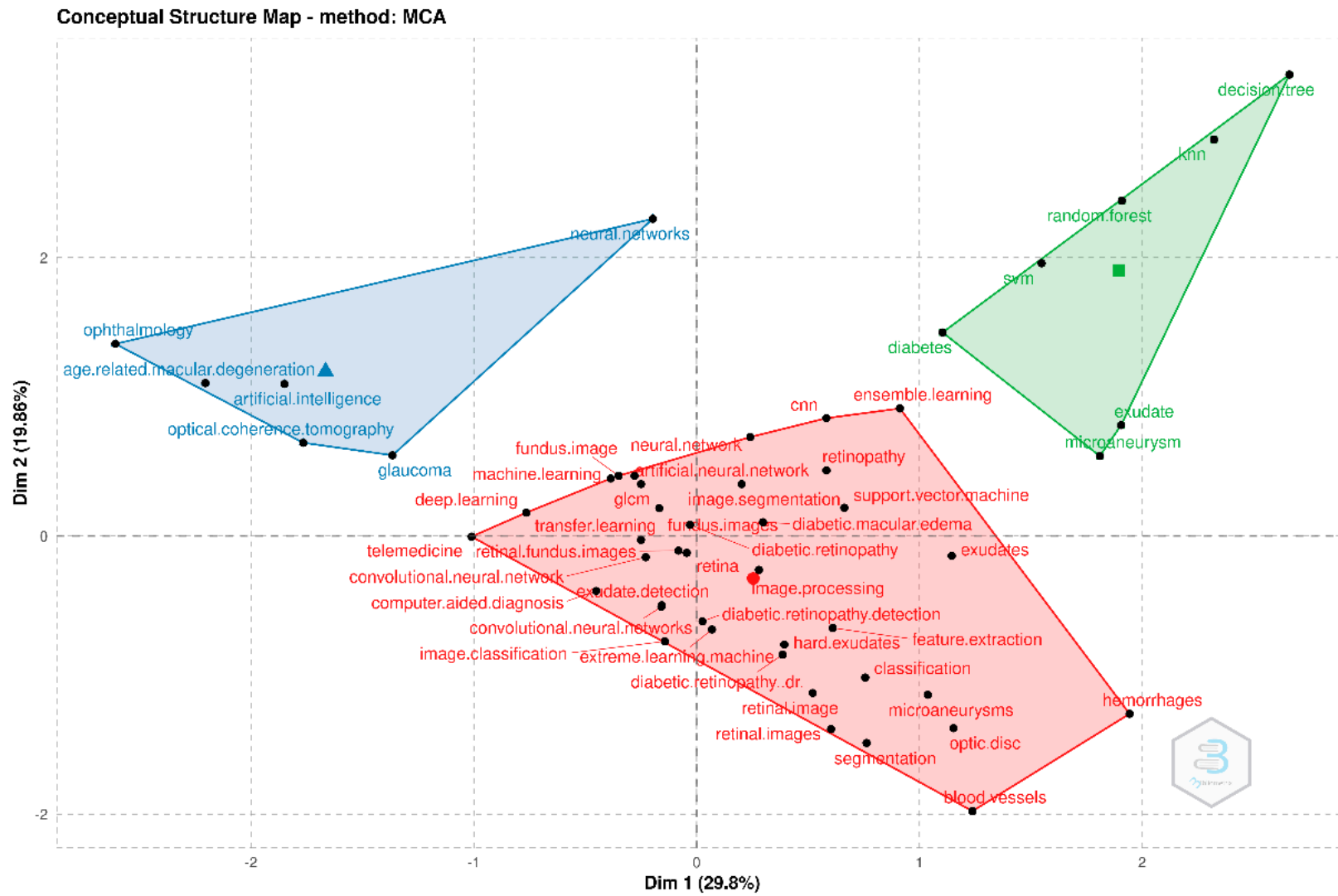


Figure 16. Factorial map.

### 3.10. Thematic Evolution Analysis

The evolution of academic publications was identified from the relationships between the keywords used in various papers over time. Here, the analysis was done in four time slices: 2000–2014, 2015–2018, 2019–2021, and 2021–2022.

These four time slices (Figure 17) were selected based on trial and error to find the trend topics. In the first time slice, most of the research was carried out on microaneurysm detection and DR classification based on traditional image processing techniques and the SVM classifier. More concentration was given to feature extraction to improve the model (SVM, CAD, ELM) performance in the second time slice. During the same period, the work slowly moved toward exudate detection, as it also forms the early sign of diabetic retinopathy. It was noticed that in the third time slice (2019–2020), people started working on random forests, convolutional neural networks, and transfer learning techniques for exudate detection. Methods such as SVM, CNN, transfer learning, and artificial intelligence were used in recent papers.

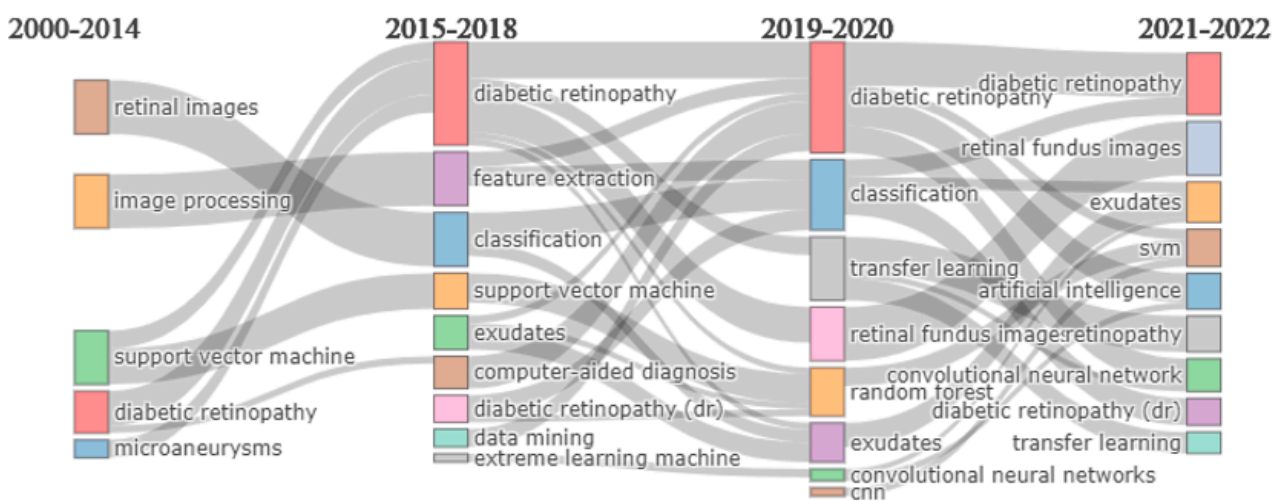


Figure 17. Thematic evolution of the author keywords.

Figure 18 shows the thematic map for the above four time slices. It manifests the keywords for each time slice under different themes. The map consists of four themes: Niche, Motor, Emerging or declining, and Basic themes. The niche theme is a well-developed and isolated theme and thus lists the keywords less important for the field. The motor theme lists the keywords that are important in the organization of a research area. The emerging or declining theme list keywords that are minimally used. The basic theme list keywords that are widely used in several fields of study.

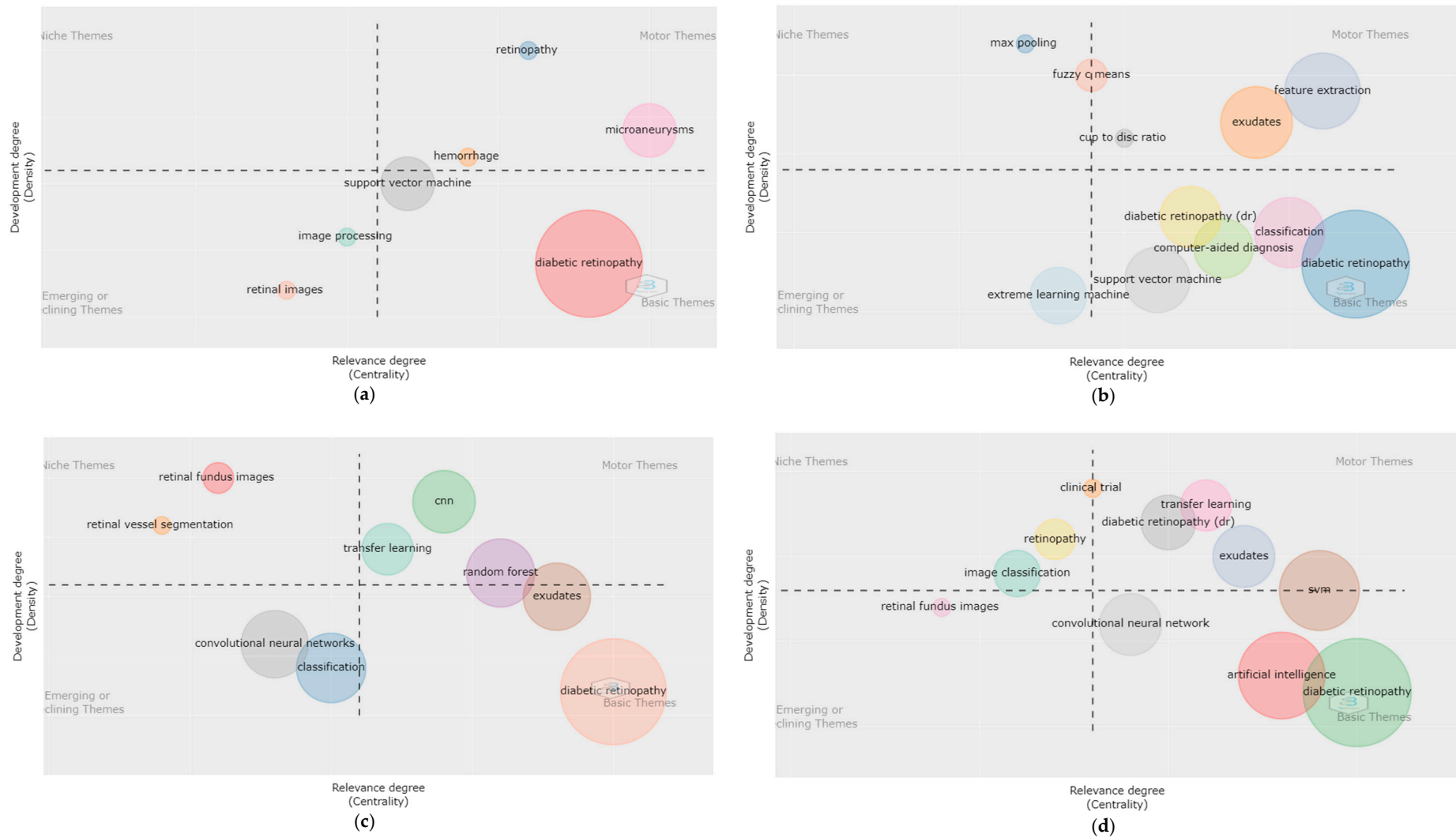


Figure 18. Thematic map of author keywords is plotted with the relevance degree and the work quantity for all four time slices shown in (a–d).

#### 4. Qualitative Analysis

In total, 811 documents based on diabetic retinopathy detection were found. These results were further refined based on annual citation rates, ensuring the paper's high quality.

Subjective analysis was done on these articles to pinpoint the different machine learning styles used in DR detection. This paper discusses the types of features used in detecting DR lesions that significantly impact the performance of detection and classification algorithms.

Most known approaches for detecting lesions rely solely on handcrafted features (HCFs), which cannot precisely characterize lesions. Therefore, new contextual and textural features, a combination of grey-level co-occurrence matrix with HCFs, and deep features with HCFs were used for efficient detection.

The lesion detection and classification can be done using different machine learning techniques. Various authors suggested different kinds of features in the literature. Handcrafted features such as conventional features [14,15], pixel-wise features and superpixel-wise features, [16–18], and deep features [19,20] were used.

##### 4.1. Diabetic Retinopathy Datasets

Many datasets are available online for retinal images to detect DR lesions and blood vessels. These datasets are generally used to train, validate, and test models. Hence, they can be used to assess the performance of a new model compared with the existing models. Many fundus images are available with varying resolutions, contrasts, etc. Fundus image datasets are tabulated in Table 4. The most commonly used datasets are DiaretDB0, DiaretDB1, e-Ophtha Ex, IDRiD, and Kaggle DRD Kaggle.

DiaretDB0 [21] is a publicly available dataset with 130 images, including 20 fundus images without DR and 110 images with DR early signs. It was collected from Kuopio University Hospital using a fundus camera with a 50-degree field of view.

The DiaretDB1 [22] database is one of the publicly available datasets containing high-quality DR retinal images annotated at the lesion level. The resolution of the retinal images is 1500 pixels by 1152 pixels with a 50-degree FoV. Out of 89 fundus images, 47 and 42 are assigned for training and testing, respectively.

E. Decenci re et al. proposed two datasets, e-Ophtha EX and e-Ophtha MA [23], consisting of retinal images. Both datasets are a collection of four different resolutions, ranging from 2544 by 1696 pixels to 1440 by 960 pixels, with a 45-degree field of view. The e-Ophtha EX has 82 retinal images, of which 35 are without DR and 47 with 12,278 exudate signs. Similarly, the other dataset, e-Ophtha MA, contains 381 images, of which 233 are without DR and 148 images with 1306 microaneurysm signs. The Indian Diabetic Retinopathy Image Dataset (IDRiD) [24] is an open-source dataset that is available online. The experts did the annotations at the pixel level. Hence, more accurate predictions can be made on DR lesions. Of 81 images, 54 are kept for training and 27 for testing with a 4288 by 2848 pixel resolution and 50-degree field of view (FoV).

The Kaggle Diabetic Retinopathy Detection challenge dataset comprises high-resolution retina photographs taken under various imaging circumstances. It contains 88,702 RGB images with varying resolutions, divided into a training set of 35,126 and a testing set of 53,576. Other freely available datasets are Messidor and Messidor-2 [25], which contain 1200 images (400 images without pupil enlargement and 800 images with pupil enlargement) and 1748 images, respectively. The Messidor dataset is divided into three equal sets (i.e., 400 images each). The resolutions of the captured images in both datasets are 1440 by 960, 2240 by 1488, or 2304 by 1536 pixels with a 45-degree FoV. These images are graded into DR stages varying from 0 to 3 based on the no. of microaneurysms and hemorrhages. DRIVE [26] and STARE [27] have 40 and 400 images, respectively. The DRIVE dataset has 20 training and 20 testing images with pixel-level annotations. In STARE, the camera was a Topcon TRV with a 35-degree FoV. The pixel-level annotations of the diverse retinal images can be found in both the e-Ophtha and IDRiD datasets, and these various retinal images help to improve the model's accuracy.

**Table 4.** Details of diabetic retinopathy datasets.

Dataset	No. of Fundus Images	Field-of-View	Training Set (No. of Images)	Test Set (No. of Images)	Normal	Abnormal	Lesions	Image Resolution	Data Source Location	Annotations	Website
DiaretDB0	130	50°	-	-	20	110	-	-	Kuopio university hospital	-	<a href="https://www.it.lut.fi/project/imageret/diaretdb0/">https://www.it.lut.fi/project/imageret/diaretdb0/</a>
DiaretDB1	89	50°	28	61	5	84	15 soft exudates, 39 microaneurysm, and 39 hemorrhages	1500 × 1152 pixels	Kuopio university hospital	-	<a href="https://www.it.lut.fi/project/imageret/diaretdb1/index.html">https://www.it.lut.fi/project/imageret/diaretdb1/index.html</a>
e-Ophtha EX	82	40°	-	-	35	47	12,278 exudates	1440 × 960 pixels to 2544 × 1696 pixels	-	Pixel level	<a href="https://www.adcis.net/en/third-party/e-ophtha/">https://www.adcis.net/en/third-party/e-ophtha/</a>
e-Ophtha MA	381	40°	-	-	233	148	1306 microaneurysms	1440 × 960 pixels to 2544 × 1696 pixels	-	Pixel level	
IDRiD	516	50°	413	103	164	81	-	4288 × 2848 pixels	Eye Clinic, Sushrusha Hospital Building, Nanded, (M.S.), India	Pixel level	<a href="https://iee-dataport.org/open-access/indian-diabetic-retinopathy-image-dataset-idrid">https://iee-dataport.org/open-access/indian-diabetic-retinopathy-image-dataset-idrid</a>
Kaggle DRD	88,702	-	35,126	53,576	65,343	23,359	-	Different resolution	-	-	<a href="https://www.kaggle.com/competitions/diabetic-retinopathy-detection/data">https://www.kaggle.com/competitions/diabetic-retinopathy-detection/data</a>
Messidor	1200	45°	-	-	540	660	-	1440 × 960, 2240 × 1488 or 2304 × 1536 pixels	-	-	<a href="https://www.adcis.net/en/third-party/messidor/">https://www.adcis.net/en/third-party/messidor/</a>
Messidor-2	1748	45°	-	-	-	-	-	1440 × 960, 2240 × 1488 or 2304 × 1536 pixels	-	-	<a href="https://www.adcis.net/en/third-party/messidor2/">https://www.adcis.net/en/third-party/messidor2/</a>
DRIVE	40	45°	20	20	33	7	-	768 × 584 pixels	-	Pixel level	<a href="https://drive.grand-challenge.org/">https://drive.grand-challenge.org/</a>
STARE	400	35°	-	-	-	-	-	605 × 700 pixels	-	-	<a href="http://cecas.clemson.edu/~ahoover/stare">http://cecas.clemson.edu/~ahoover/stare</a>

#### 4.2. Steps in Diabetic Retinopathy Detection

Generally, the steps involved in diabetic retinopathy detection and classification are shown in Figure 19. In image segmentation, retinal landmarks, such as the optic disc [28,29] and blood vessels [30,31] are removed to make lesion segmentation feasible.

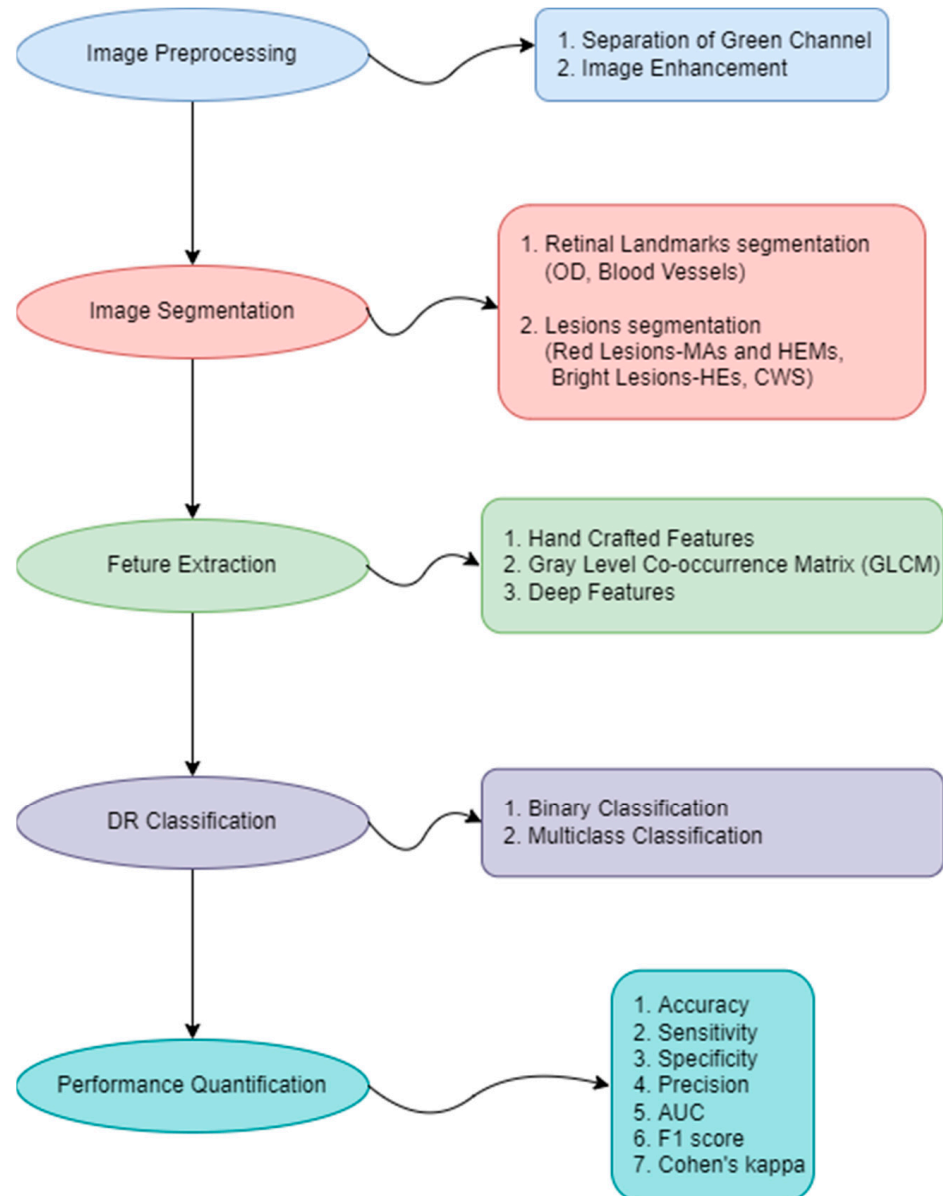


**Figure 19.** Steps in diabetic retinopathy detection.

#### 4.3. Image Segmentation

Image segmentation (Figure 20) can be broadly categorized into traditional and machine learning approaches. The traditional approach includes threshold-based, morphological-based, region-based, and clustering-based image segmentation, which are listed in Table 5 with the datasets that they used.

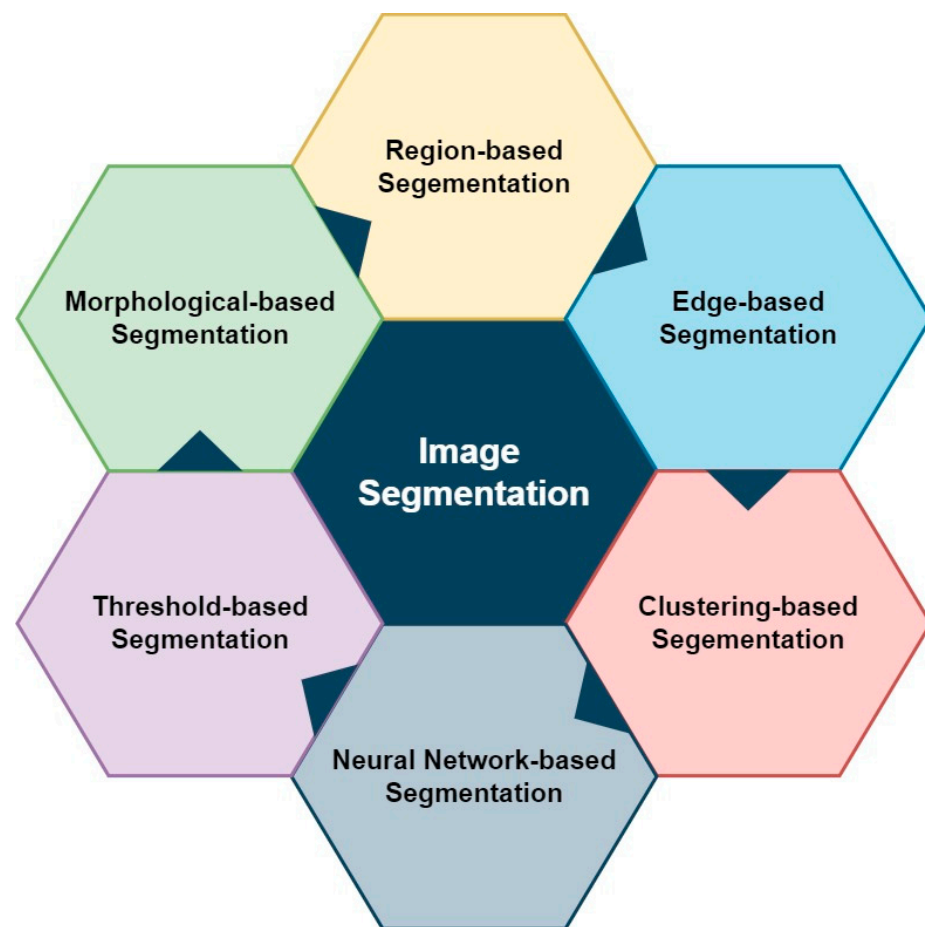


**Figure 20.** Image segmentation.

#### 4.3.1. Threshold-Based Segmentation

The segmentation of exudates was implemented using dynamic decision thresholding and adaptive image quantization by Kaur et al. [6]. Since the threshold value is dynamically selected for the low-contrast images with a large diversity, this leads to robustness. Using the Otsu algorithm [17,32] the value for adaptive thresholding, i.e.,  $T$ , is selected. The histogram-based locus detection method [33] is used on an image to segment lesions. Optic disc and blood vessel pixels are irrelevant, and thus, removed using the Hough transform and a matched filter, respectively.

#### 4.3.2. Morphological-Based Segmentation

Morphological-based segmentation is one of the most commonly used methods for segmentation. At first, the image pre-processing is done by extracting the green channel, and then lesion candidates are computed using morphological operations [15]. Morphological component analysis [34] is used to separate different components that have anatomically distinct shapes in an image. Mathematical morphological methods were assessed by several authors [35] and applied to fundus images for lesion segmentation after pre-processing using the Gabor filter, median filter, etc.

#### 4.3.3. Region-Based Segmentation

The region is grown pixel by pixel in a recursive manner from a randomly selected seed point based on similarities and 4- or 8-connectivity with neighboring pixels [36] in a recursive way. This method generally leads to over-segmentation. The watershed transform [37] and circular hough transform [38] removes a bright optic disc resembling the anatomical structure.

**Table 5.** Image segmentation methods used in the literature.

Author (Year)	Publication	Dataset	Lesion	Segmentation Technique
Kaur et al. (2017) [6]	Biocybernetics and Biomedical Engineering	Stare, Messidor, DiaretDB1 and e-Ophtha EX	EX	Threshold-based segmentation
Akram et al. (2014) [14]	Computers in Biology and Medicine	Messidor, Hamilton Eye Institute Macular Edema (HEI-MED)	EX	Thresholding based segmentation
Zhang X. et al. (2014) [15]	Medical Image Analysis	e-Ophtha EX	EX	Morphological top-hat
Sopharak et al. (2009) [17]	Sensors	Thammasat university hospital	EX	Fuzzy Cmeans (FCM) clustering
Huang C. et al. (2020) [18]	Neurocomputing	DiaretDB1, e-Ophtha EX and IDRiD	EX	Simple Linear Iterative Clustering (SLIC)
Wang H. et al. (2020) [28]	Computer Methods and Programs in Biomedicine	e-Ophtha, HEI-MED	EX	Morphological
Badgular et al. (2019) [32]	IRBM	STARE		Otsu's segmentation method
Yadav et al. (2021) [33]	Measurement	e-Ophtha	MA	Locus detection method
Imani E et al. (2016) [34]	Computer Methods and Programs in Biomedicine	DiaretDB, HEI-MED and e-Ophtha	EX	Morphological
Amin et al. (2017) [35]	Journal of Computational Science	e-Ophtha, Messidor	EX	Component Analysis
Mahendran et al. (2015) [36]	Computers & Electrical Engineering	Messidor	EX	Mathematical Morphology
Kumar S. et al. (2019) [37]	Optics & Laser Technology	Diaretdb1 and Diaretdb0	EX	Region based segmentation
Adem et al. (2018) [38]	Expert Systems with Applications	DiaretDB0, DiaretDB1 and DrimDB	EX	Watershed transform
Adal et al. (2013) [39]	Computer methods and programs in biomedicine	Retinopathy Online Challenge (ROC), University of Tennessee Health Science Center (UTHSC)	MA	Circular Hough transform
Garifullin et al. (2021) [40]	Computers in biology and Medicine	IDRiD	HE, SE, HEM, MA	Hessian Operator
Xia H. et al. (2021) [41]	Knowledge-Based Systems	e-Ophtha	MA	Bayesian lesion segmentation
He W. et al. (2021) [42]	Information Fusion	Private Dataset	EX, HEM	Multiscale Residual Network (MSRNet)
				VGG-based U-Net

#### 4.3.4. Edge-Based Segmentation

First-order and second-order derivation filters can extract high frequencies from an image. Adal et al. [39] computed the second-order partial derivatives using the Hessian matrix, and later, microaneurysms were detected using Retinopathy Online Challenge (ROC) and University of Tennessee Health Science Center (UTHSC).

#### 4.3.5. Clustering-Based Segmentation

Clustering-based segmentation is a method that finds similar pixels based on the distance, such as Euclidean distance and Manhattan distance, etc., from centroids and forms into groups or clusters. All elements within one cluster will look closer to each other than the elements in the other clusters. Huang C. et al. [18] extracted 25 features at the pixel level and super-pixel level and Sopharak et al. [17] selected four features: intensity, hue, standard deviation, and hue from contrast-enhanced images using simple linear iterative clustering and fuzzy C-means clustering methods, respectively. The initial centroid, which is randomly chosen, and the presence of noise may lead to poor segmentation.

#### 4.3.6. Neural-Network-Based Segmentation

Technology innovation has been increasing rapidly, especially in machine learning, leading to its usage in medical fields. Machine algorithms require a neural network architecture to implement that is basically used in classification and clustering problems. Researchers are now extensively using neural networks for the same reason.

Garifullin et al. [40] performed MAs, EX, and HEM segmentation using the Bayesian lesion segmentation method with a dense, fully connected architecture. Xia H. et al. [41] worked on a multi-scale residual network (MSRNet). He W. et al. [42] proposed an incremental pattern-based segmentation that refines the information obtained from the already trained model and applies it to the present model. In the feature extraction step, various features are extracted, such as the intensity, geometric and textural features, grey-level co-occurrence matrix (GLCM) [36], and deep features [42]. These features are given as input to a machine learning classifier, which classifies DR lesions.

#### 4.4. Machine Learning Styles

Machine learning techniques are broadly classified as supervised and unsupervised machine learning techniques. The former classifier requires training data to fit a model for the given data and can be used to classify diabetic retinopathy. In contrast, no training data is necessary for the latter classifier. Since the research focuses on the health of diabetics, the classification algorithms used to detect the disease must provide accurate results. The various machine learning styles for DR classification are given in Figure 21.



Figure 21. Machine learning styles for DR classification.

#### 4.4.1. Supervised Learning

Table 6 shows a list of studies that used supervised learning styles. Few authors [15,28,29,43] have used the random forest algorithm to classify exudate and non-exudate patches among the candidates. Mahendran et al. [36] worked with low-contrast images to detect and localize exudates using a neighborhood-based segmentation technique. The classification of retinopathy was done using support vector machine (SVM) and probabilistic neural network (PNN) classifiers and their results were compared.

**Table 6.** Supervised machine learning styles used in the literature.

Author (Year)	Publication	Dataset	Lesion	Features Extracted	Classifier
Zhang X. et al. (2014) [15]	Medical Image Analysis	e-Ophtha EX	EX	HCF	Random Forest
Wang H. et. al. (2020) [28]	Computer Methods and Programs in Biomedicine	e-Ophtha, HEI-MED	EX	HCF and Deep Features	Random Forest
Orlando et al. (2017) [29]	Computer Methods and Programs in Biomedicine	DIARETDB1 and e-Ophtha	MA and HEM	HCF and Deep Features	Random Forest
Badgujar et al. [32]	IRBM	STARE	EX	HCF	SMO-GBM classifier k-NN, SVM, Naive Bayes, Decision Tree, and Random Forest
Yadav et al. (2021) [33]	Measurement	e-Ophtha	MA	HCF	HCF
Amin et al. (2017) [35]	Journal of Computational Science	e-Ophtha, Messidor	EX	HCF	SVM
Mahendran et al. (2015) [36]	Computers & Electrical Engineering	Messidor	EX	HCF	SVM, PNN
Shailesh et al. (2029) [37]	Optics & Laser Technology	DiaRetDB1 and DiaRetDB0	MA, HEM	HCF	RBF NN
Liu et al. (2017) [43]	Computerized Medical Imaging and Graphics	e-Ophtha EX, DiaRetDB1	EX	HCF	Random Forest
Du J. et al. (2020) [44]	Computer Methods and Programs in Biomedicine	e-Ophtha-MA, DiaretDB1 and ROC	MA	HCF	RUSBoost using Decision Tree Classifier

Yadav et al. [33] and Amin et al. [35] compared the performance of three classifiers, namely, kNN, SVM, and PNN, and found that SVM had the best accuracy among these three classifiers. An ensemble classifier is a classifier that combines two or more models to take advantage of the performances of all models, thereby increasing the accuracy.

A radial basis function neural network [37] was trained using the features extracted from hemorrhages and microaneurysm segmented regions. A hybrid nature-inspired Hybrid Spider monkey optimization-Gradient boosting machines classifier (SMO-GBM) classifier was proposed by Badgujar et al. [32] for exudate-based DR classification. A combination of RUS (random under-sampling) and AdaBoost [44] was used as a classifier for MA detection, overcoming the problem of imbalanced data.

#### 4.4.2. Unsupervised Learning

The unsupervised learning method (Table 7) works on unlabeled data, which is beneficial since labeling is tedious and costly. It groups the pixels based on their similar characteristics.

Kaur et al. [6] developed an adaptive k-means quantization method to form clusters based on the varying intensities of colors in retinal fundus images, whereas Huang C. et al. [18] used the simple linear iterative clustering (SLIC) method, which provides an alternative representation of fundus images. This representation reduces noise and forms a basis for fast and precise diagnoses of exudates. The fuzzy C-means clustering technique and morphological operators were used by Sopharak et al. [17] to segment exudates. Exudates and optic discs appear bright, making classification difficult. Akram et al. [14] have used a combination of gaussian mixed model (GMM) and m-mediods classifier which took the advantage of the best properties of both models.

**Table 7.** Unsupervised machine learning styles used in the literature.

Author (Year)	Publication	Dataset	Lesion	Features Extracted	Classifier
Kaur et al. (2017) [6]	Biocybernetics and Biomedical Engineering Computers in	STARE, Messidor, DiaretDB1 and e-Optha EX	EX	Shape and Intensity features	k-means
Akram et al. (2014) [14]	Biology and Medicine	DRIVE, STARE, DiaretDB, Messidor	MA, EX	HCF	GMM and m-Mediods based classifier
Sopharak et al. (2009) [17]	Sensors	Thammasat university hospital	EX	HCF	Fuzzy Cmeans (FCM) clustering
Huang C. et al. (2020) [18]	Neurocomputing	DiaretDB1, e-Optha EX and IDRiD	EX	Pixel and super pixel level features	SLIC, CNN

#### 4.4.3. Semi-Supervised Machine Learning Style

The supervised machine learning style is costly due to the hand-labeling process, which is overcome by the semi-supervised machine learning style. The latter approach (Table 8) will work even for less labeled data.

**Table 8.** Semi-supervised learning styles used in the literature.

Author (Year)	Publication	Dataset	Lesion	Features Extracted	Classifier
Adal et al. (2014) [39]	Computer methods and programs in medicine	ROC, UTHSC	MA	Scale-Space features, SURF features, Radon features	SVM, KNN, Naïve Bayes, RF
Cao et al. (2018) [45]	Computerized Medical Imaging and Graphics	Messidor	MA	HCF (37)	Multi-kernel classifier

Less labeled and unlabeled data can be used to train this model. To the best of our knowledge, Adal et al. [39] and Cao et al. [45] implemented this learning method using well-known SVM, kNN, naïve Bayes, RF, and multi-kernel classifiers.

#### 4.4.4. Ensemble Learning Approach

This method aims to amalgamate the decisions obtained from different models and classify an unseen image. Thus, this gleaned classifier (Table 9) gives better accuracy. The ensemble model is obtained by combining other traditional models. Based on the combining method, an ensemble is classified into a stacking, blending, bagging, or boosting type. The optimal solution was obtained by integrating the decision tree output using the bootstrap method based on voting [46], and RUSBoost [44]. Ignacio Orlando et al. [29] ensembled both HCF and deep features. A bootstrapped decision-tree-based ensemble classifier was used to classify exudate pixels and non-exudate pixels [47].

#### 4.4.5. Deep Learning Approach

Deep learning (Table 10), which is a subset of machine learning, extracts lines and edges in the initial layers and deep features in the later layers using convolution operations. As a result, it is now playing an essential role in DR detection.

**Table 9.** Ensemble learning styles used in the literature.

Author (Year)	Publication	Dataset	Lesion	Features Extracted	Classifier
Orlando et al. (2017) [29]	Computer Methods and Programs in Biomedicine	DIARETDB1 and e-optha	MA, HEM	HCF and Deep Features	Random Forest
Du J. et al. [44]	Computer Methods and Programs in Biomedicine	e-Ophtha-MA, DiaretDB1 and ROC	MA	HCF	Decision Tree
Fraz et al. (2017) [46]	Biomedical Signal Processing and Control	DIARETDB1, e-Ophtha EX, HEI-MED and Messidor	EX	HCF	Decision Tree
Zhang W. et al. (2019) [47]	Knowledge-Based Systems	Sichuan Provincial Peoples Hospital	EX	Deep Features	Pretrained model and Standard Deep neural network

**Table 10.** Deep learning styles used in the literature.

Author (Year)	Publication	Dataset	Lesion	Features Extracted	Classifier
Huang C. et al. (2020) [18]	Neurocomputing	DiaretDB1, e-Ophtha (EX) and IDRiD	EX	Pixel and super pixel level features	CNN
Wang H. et al. (2020) [28]	Computer Methods and Programs in Biomedicine	e-Ophtha, HEI-MED	EX, MA, HEM, CWS	HCF and Deep features	CNN
Adem et al. (2018) [38]	Expert Systems with Applications	DiaretDB0, DiaretDB1 and DrimDB	EX	Deep features	CNN
Xia H et al. (2021) [41]	Knowledge-Based Systems	e-optha	MA	Deep features	MS-EfficientNet
Liao (2021) [48]	Biocybernetics and biomedical engineering	ROC, e-Ophtha (MA)	MA	Deep Features	UNet
Sandhya et al. (2021) [49]	Materials Today: Proceedings	Kaggle dataset	EX, MA, HEM, CWS	HCF	Context unit based Deep Learning NN
Sambyal et al. (2020) [50]	Biocybernetics and biomedical engineering	IDRiD and e-Ophtha	EX, MA	Deep features	Modified U-Net architecture

The optic disc was segmented using circular Hough transformation from fundus images, and CNNs [18,38,48] were used to automatically detect exudates. The super-pixel is another image representation used to extract features and classify retinopathy stages.

Wang H. et al. [28] suggested a method for exudate identification using a deep convolutional neural network (DCNN). They used a morphological approach to segment exudates; then, multiple features were extracted and classified using a random forest. Lesion identification and DR grading are done using DCNN [41]. Sandhya et al. [49] proposed context unit-based deep neural networks to recognize DR using a fully connected CNN to extract multi-features faster.

U-Net architecture is mainly used for semantic segmentation. It consists of encoder and decoder paths. Modified U-Net [50] uses ResNet34 architecture (four blocks) in the encoder path and four U-Net decoder blocks. The use of ResNet blocks increases the accuracy of DR detection.

#### 4.4.6. Transfer Learning Approach

The application of knowledge obtained by completing one task and using it in solving some related problem is known as transfer learning. It is classified as a pre-trained model and is used to develop model-based approaches. Table 11 shows a summarization of transfer learning approaches used in the literature.

**Table 11.** Transfer learning styles used in the literature.

Author (Year)	Publication	Dataset	Lesion	Features Extracted	Classifier
Samanta et al. (2020) [19]	Pattern Recognition Letters	Kaggle dataset	EX	Deep Features	Inception, Xception, VGG16, ResNet-50, DenseNet and AlexNet
Saxena et al. (2020) [20]	Intelligence based medicine	EyePACS, Messidor1, Messidor2	MA, HEM, EX, CWS	Deep features	Inception V3 and Inception, ResNet
He W. et al. (2021) [42]	Information Fusion	Private Dataset	EX	Deep features	VGG-based U-Net InceptionV3, Xception and Inception, ResNetV2
Zhang W. et al (2019) [47]	Knowledge-Based Systems	Sichuan Provincial Peoples Hospital	EX	Deep features	Inception, ResNetV2
Sugeno et al. (2021) [51]	Computers in Biology and Medicine	Little flower hospital, DIARETDB, STARE, e-ophtha, ROC, Diabetic Retinopathy Dataset	MA, HEM, EX, CWS	Deep features	Inception V3 and Xception
Khojasteh et al. (2018) [52]	Computers in Biology and Medicine	DiaretDB1, e-Ophtha EX	EX	Deep Features	ResNet50

Pixel-wise segmentation is always intense labor work, which is generally used in instance segmentation. Liao et al. [48] overcame this difficulty by using data with fewer annotations and extracted knowledge of the previous model to improve the performance of their model. The weights of online pre-trained models are used at the initial layers of their model and the user are free to choose the later layers per their requirement, thus increasing the new model's performance [44]. The pre-trained CNN models, such as ResNet50 [19,20,47], Xception [19,47,51], Inception [19,20,47,51] and VGG16 [42] were used for segmentation and classified using a multiclass SVM ensemble classifier.

#### 4.5. Performance Measures

Generally, accuracy is the most common metric used to test a model's performance. It tells us how well a model performed on the entire data set, but it does not tell us how much is correctly predicted out of the DR and no DR categories. Thus, a confusion matrix is used. One can find sensitivity, specificity, precision, and negative prediction value from this confusion matrix. Sensitivity (true positive rate) and specificity show how well our model has performed. It is obtained by predicting true positive out of total positive cases and true negative out of total negative cases. The precision reveals how much is correctly predicted out of the model's positive predictions, and the negative prediction value reveals how much is correctly predicted out of negative predictions made by the model. Researchers also evaluate their model's performance using the F1 score, area under curve (AUC), Cohen's score, etc., as shown in Table 12.

**Table 12.** Performance metrics achieved by various authors.

Author (Year)	Lesion	Accuracy	Sensitivity	Specificity	Precision	Recall	F1-Score	AUC	Cohen’s Kappa Score
Akram et al. (2014) [14]	EX	Messidor: 97.59%, DRIVE: 94.03%, STARE: 97.89%, DiaretDB0: 92.96%	Messidor: 97.61%, DRIVE: 94.26%, STARE: 98.79%, DiaretDB0: 93.08%	Messidor: 97.03%, DRIVE: 94.74%, STARE:97.43%, DiaretDB0: 92.76%	-	-	-	-	-
Zhang X et al. (2014) [15]	EX	-	-	-	-	-	-	e-optha EX: 0.95	-
Sopharak et al. (2009) [17]	EX	Private dataset: 99.11%	Private dataset: 87.28%	Private dataset: 99.24%	Private dataset: 42.77%	-	-	-	-
Huang et al. (2020) [18]	HE	e-optha: 97.58%, IDRiD: 98.19%	e-Ophtha: 97.96%, IDRiD: 98.40%	e-Ophtha: 90.84%, IDRiD: 90.67%	-	-	-	e-Ophtha: 0.9682, IDRiD: 0.9674	-
Samanta et al. (2020) [19]	HEM, MA	-	-	-	-	-	-	-	Kaggle dataset: 0.8836
Saxena et al. (2020) [20]	All	-	Messidor: 88.84%, Messidor-2: 81.02%	Messidor: 89.92%, Messidor-2: 86.09%	-	-	-	Messidor: 0.958, Messidor-2: 0.92	-
Wang H. et al. (2020) [28]	HE	-	-	-	-	-	e-Ophtha: 0.8929, HEI-MED: 0.9326	e-Ophtha: 0.9644, HEI-MED: 0.9323	-
Orlando et al. (2017) [29]	MA	-	Messidor: 0.9109 DiaretDB0: 89.01%, HEI-MED: 81.26%, e-Ophtha: 80.32%	- DiaretDB0: 99.93%, HEI-MED: 99.81%, e-Ophtha: 99.83%	- DiaretDB0: 82.64%, HEI-MED: 63.57%, e-Ophtha: 77.28%	-	-	Messidor: 0.8932	-
Imani et al. (2016) [34]	EX	-	-	-	-	-	-	DiaretDB: 0.961, HEI-MED: 0.948, e-Ophtha: 0.937	-
Amin et al. (2017) [35]	EX	Seven publicly available dataset: 98.58%	-	-	-	-	-	Seven publicly available dataset: 0.98	-
Mahendran et al. (2015) [36]	MA	Messidor: 97.89%	Messidor: 98.68%	Messidor: 100%	-	-	-	-	-
Garifullin et al. (2021) [40]	All	-	-	-	-	-	-	IDRiD: 0.84	-
Liu et al. (2016) [43]	EX	-	e-Optha EX: 76%	-	e-Optha EX: 75%	-	e-Optha EX: 76%	-	-

Table 12. Cont.

Author (Year)	Lesion	Accuracy	Sensitivity	Specificity	Precision	Recall	F1-Score	AUC	Cohen’s Kappa Score
Fraz et al. (2017) [46]	EX	DiaretDB1: 0.87, e-Ophtha (EX): 0.89, HEI-MED: 0.95, Messidor: 0.98	-	-	-	-	-	DiaretDB1: 0.9310, e-Ophtha: 0.9403, HEI-MED: 0.9842, Messidor: 0.9996	-
Zhang W. et al. (2019) [47]	All	-	-	-	Private dataset: 0.97	Private dataset: 0.98	Private dataset: 0.97	-	-
Khojasteh et al. (2018) [52]	EX	DiaretDB1: 98.2%, e-Ophtha: 97.6%	DiaretDB1: 0.99, e-Ophtha: 0.98	DiaretDB1: 0.96, e-Ophtha: 0.95	-	-	-	-	-
Sugeno et al. (2021) [51]	All	DiaretDB1: 0.842	DiaretDB1: 0.985	DiaretDB1: 0.988	-	-	-	-	-
Gayathri et al. (2020) [53]	All	Three publicly available dataset: 99.89%	-	-	-	-	-	-	Three publicly available dataset: 0.994
Deepa et al. (2021) [54]	All	Private dataset: 96.20%	-	-	-	-	-	-	-

From the table, it is observed that Sopharak et al. [17], Akram et al. [14], Amin et al. [35], and Khojasteh et al. [52] achieved good accuracies with 99.11%, 98.4%, 98.5%, and 98.2%, respectively. Out of them, Akram et al. and Khojasteh et al. achieved good sensitivity and specificity. Akram et al. obtained a sensitivity of 97.61% and specificity of 97.03% using an ensemble of gaussian mixture model and m-medoids for exudate detection on the Messidor dataset. Khojasteh et al. obtained a sensitivity of 99% and a specificity of 96% using ResNet50 with SVM on DIARET DB1.

Sopharak et al. [17] created their own dataset using a KOWA-7 non-mydratic retinal camera and obtained this good result by segmenting exudates using fuzzy C-means clustering. Amin et al. [35] achieved a good area under curve (AUC) with better accuracy. They segmented exudates and used statistical and geometrical features to classify DR and no DR using kNN, probabilistic, tree-based, and SVM methods on publicly available datasets (DiaretDB1, DRIVE, e-Ophtha EX, Messidor). The Gaussian SVM outperformed using DiaretDB1 dataset.

Mahendran et al. [36] achieved a 97.89% accuracy, 98.68% sensitivity, and 100% specificity using an SVM on the MESSIDOR dataset, i.e., this study achieved superior results in terms of sensitivity and specificity.

Many studies were conducted to detect other lesions, such as microaneurysms and hemorrhages, along with exudates and classify diabetic retinopathy. Author Deepa et al. [54] have achieved 96.2% accuracy with all lesions but Gayathri et al. [53] procured excellent results with 99.89% accuracy for DR–No DR classification.

## 5. Discussion and Observations

Two popular databases, namely, Scopus and Web of Science, were used to select papers based on the query already mentioned regarding the data collection under the Methods and Materials section.

Deeper and broader insights were provided through quantitative and qualitative analysis. Both analyses were necessary since they help to form hypotheses for research. Quantitative analysis was done using Excel, VOSviewer, and Biblioshiny. Such a study aims toward and can aid in the evaluation of theories. The qualitative analysis was done regarding a dataset, image segmentation methods, and different machine learning styles ranging from traditional ML styles to deep learning styles used in the literature. It aids researchers in better understanding the automated diabetic retinopathy detection system's motives, necessity, methodology, and justifications. It provides deep insights into various kinds of datasets and suitable methods.

Most researchers used publicly available datasets, and few used private datasets collected from the hospital. However, in either case, the issues were as follows:

- (i) First, all images collected belonged to a single modality and were captured from one particular device from one hospital. To overcome such issues, images must be captured from different devices under different circumstances, and multimodal images, such as OCT and fundus images, may be used.
- (ii) Second, fewer DR images may lead to overfitting. Thus, the size of the dataset must be increased, or alternative ML styles, such as semi-supervised, self-supervised, and co-learning techniques, may be used to produce a good model with better performance.
- (iii) The third issue may be due to imbalance, i.e., a biased dataset, which may be avoided by adequately collecting DR images.

In addition to the above, there may be issues of non-uniform illumination and low contrast. Since the eye structure is spherical, it leads to brightness at the center and becomes darker in the surrounding.

Thus, a robust classification model with high accuracy and speed could be possible that considers these points, and hence, can be deployed on a server to be used by ordinary people.

Various image segmentation and ML styles are discussed in this paper. For better segmentation and classification, useful features must be extracted, such as the intensity,

statistical, textural, grey-level co-occurrence matrix, moments, standard deviation, and deep features (pixel level and super-pixel level) in the R, G, B, and intensity channels for both greyscale and color images.

## 6. Conclusions

This paper presents a literature review of different machine learning styles for diabetic retinopathy detection. It discusses datasets and the selected papers based on image segmentation, traditional ML styles, DL methods, and the parameters used for quantifying the performance of various classification models.

It also explores statistical data in DR detection and classification. The quantitative analysis was based on the Scopus and WoS databases from 2000 to 2021, with 811 documents published in various journals and conferences, including different kinds of funding received by researchers worldwide working with other organizations. It was observed that various research studies were carried out using supervised learning and, recently, deep learning. Future work can be focused on working with a balanced and multimodal dataset. The second point is to use semi-supervised, self-supervised, and co-learning techniques with deep neural networks. This paper may help researchers to narrow the research spectrum and form hypotheses by identifying the gaps.

**Author Contributions:** Conceptualization, S.S., S.M. and S.P.; methodology, S.S., S.M. and S.P.; software, S.S., S.M. and S.P.; validation, S.S., S.M. and S.P.; formal analysis, S.S.; investigation, S.S. and S.M.; resources, S.S.; data curation, S.S., S.M., S.P., K.S. and E.A.; writing—original draft preparation, S.S.; writing—review and editing, S.S., S.M., S.P., K.S. and E.A.; visualization, S.S.; supervision, S.M., S.P., K.S. and E.A.; project administration, S.M., S.P., K.S. and E.A. All authors have read and agreed to the published version of the manuscript.

**Funding:** This work was supported by the Research Support Fund (RSF) of Symbiosis International (Deemed University), Pune, India.

**Institutional Review Board Statement:** Not applicable.

**Informed Consent Statement:** Not applicable.

**Data Availability Statement:** Not applicable.

**Conflicts of Interest:** The authors declare no conflict of interest.

## References

1. Teo, Z.L.; Tham, Y.C.; Yu, M.; Chee, M.L.; Rim, T.H.; Cheung, N.; Bikbov, M.M.; Wang, Y.X.; Tang, Y.; Lu, Y.; et al. Global prevalence of diabetic retinopathy and projection of burden through 2045: Systematic review and meta-analysis. *Ophthalmology* **2021**, *128*, 1580–1591. [CrossRef] [PubMed]
2. Vashist, P.; Senjam, S.S.; Gupta, V.; Manna, S.; Gupta, N.; Shamanna, B.R.; Bhardwaj, A.; Kumar, A.; Gupta, P. Prevalence of diabetic retinopathy in India: Results from the National Survey 2015–19. *Indian J. Ophthalmol.* **2021**, *69*, 3087. [CrossRef] [PubMed]
3. Available online: <https://timesofindia.indiatimes.com/city/chandigarh/burden-of-retinal-diseases-caused-by-diabetes-on-the-rise-pgi-doc/articleshow/87690561.cms> (accessed on 14 November 2021).
4. Kaur, J.; Mittal, D. A generalized method for the detection of vascular structure in pathological retinal images. *Biocybern. Biomed. Eng.* **2017**, *37*, 184–200. [CrossRef]
5. Koetting, C. *The Four Stages of Diabetic Retinopathy*; Modern Optometry: Fairfax, VA, USA, 2019; pp. 21–24.
6. Kaur, J.; Mittal, D. A generalized method for the segmentation of exudates from pathological retinal fundus images. *Biocybern. Biomed. Eng.* **2018**, *38*, 27–53. [CrossRef]
7. Shinde, R.; Patil, S.; Kotecha, K.; Ruikar, K. Blockchain for securing ai applications and open innovations. *J. Open Innov. Technol. Mark. Complex.* **2021**, *7*, 189. [CrossRef]
8. Munim, Z.H.; Dushenko, M.; Jimenez, V.J.; Shakil, M.H.; Imset, M. Big data and artificial intelligence in the maritime industry: A bibliometric review and future research directions. *Marit. Policy Manag.* **2020**, *47*, 577–597. [CrossRef]
9. Gulshan, V.; Peng, L.; Coram, M.; Stumpe, M.C.; Wu, D.; Narayanaswamy, A.; Venugopalan, S.; Widner, K.; Madams, T.; Cuadros, J.; et al. Development and validation of a deep learning algorithm for detection of diabetic retinopathy in retinal fundus photographs. *JAMA* **2016**, *316*, 2402–2410. [CrossRef]
10. Saha, R.; Chowdhury, A.R.; Banerjee, S. Diabetic retinopathy related lesions detection and classification using machine learning technology. In Proceedings of the International Conference on Artificial Intelligence and Soft Computing, Zakopane, Poland, 12–16 June 2016; Springer: Cham, Switzerland, 2016; pp. 734–745.

11. Antal, B.; Lázár, I.; Hajdu, A.; Török, Z.; Csutak, A.; Pető, T. A multi-level ensemble-based system for detecting microaneurysms in fundus images. In Proceedings of the 4th International Workshop on Soft Computing Applications, Arad, Romania, 15–17 July 2010; pp. 137–142.
12. Quellec, G.; Lamard, M.; Cazuguel, G.; Cochener, B.; Roux, C. Wavelet optimization for content-based image retrieval in medical databases. *Med. Image Anal.* **2010**, *14*, 227–241. [[CrossRef](#)]
13. Mori, Y.; Kuroda, M.; Makino, N. Variable Selection in Multiple Correspondence Analysis. In *Nonlinear Principal Component Analysis and Its Applications*; Springer: Singapore, 2016; pp. 31–45.
14. Akram, M.U.; Khalid, S.; Tariq, A.; Khan, S.A.; Azam, F. Detection and classification of retinal lesions for grading of diabetic retinopathy. *Comput. Biol. Med.* **2014**, *45*, 161–171. [[CrossRef](#)]
15. Zhang, X.; Thibault, G.; Decencière, E.; Marcotegui, B.; Laè, B.; Danno, R.; Cazuguel, G.; Quellec, G.; Lamard, M.; Massin, P.; et al. Exudate detection in color retinal images for mass screening of diabetic retinopathy. *Med. Image Anal.* **2014**, *18*, 1026–1043. [[CrossRef](#)]
16. Perdomo, O.; Otalora, S.; Rodríguez, F.; Arevalo, J.; González, F.A. A novel machine learning model based on exudate localization to detect diabetic macular edema. In Proceedings of the Ophthalmic Medical Image Analysis Third International Workshop, Athens, Greece, 21 October 2016; pp. 137–144.
17. Sopharak, A.; Uyyanonvara, B.; Barman, S. Automatic exudate detection from non-dilated diabetic retinopathy retinal images using fuzzy c-means clustering. *Sensors* **2009**, *9*, 2148–2161. [[CrossRef](#)] [[PubMed](#)]
18. Huang, C.; Zong, Y.; Ding, Y.; Luo, X.; Clawson, K.; Peng, Y. A new deep learning approach for the retinal hard exudates detection based on super-pixel multi-feature extraction and patch-based CNN. *Neurocomputing* **2021**, *452*, 521–533. [[CrossRef](#)]
19. Samanta, A.; Saha, A.; Satapathy, S.C.; Fernandes, S.L.; Zhang, Y.D. Automated detection of diabetic retinopathy using convolutional neural networks on a small dataset. *Pattern Recognit. Lett.* **2020**, *135*, 293–298. [[CrossRef](#)]
20. Saxena, G.; Verma, D.K.; Paraye, A.; Rajan, A.; Rawat, A. Improved and robust deep learning agent for preliminary detection of diabetic retinopathy using public datasets. *Intell.-Based Med.* **2020**, *3*, 100022. [[CrossRef](#)]
21. Kauppi, T.; Kalesnykiene, V.; Kamarainen, J.K.; Lensu, L.; Sorri, I.; Uusitalo, H.; Kälviäinen, H.; Pietilä, J. DIARETDB0: Evaluation database and methodology for diabetic retinopathy algorithms. In *Machine Vision and Pattern Recognition Research Group*; Lappeenranta University of Technology: Lappeenranta, Finland, 2006; Volume 73, pp. 1–17.
22. Kauppi, T.; Kalesnykiene, V.; Kamarainen, J.K.; Lensu, L.; Sorri, I.; Raninen, A.; Kälviäinen, H.; Pietilä, J. The diaretdb1 diabetic retinopathy database and evaluation protocol. In Proceedings of the BMVC 2007, Warwick, UK, 10–13 September 2007; Volume 1, pp. 1–10.
23. Decenciere, E.; Cazuguel, G.; Zhang, X.; Thibault, G.; Klein, J.C.; Meyer, F.; Marcotegui, B.; Quellec, G.; Lamard, M.; Danno, R.; et al. TeleOphtha: Machine learning and image processing methods for teleophthalmology. *IRBM* **2013**, *34*, 196–203. [[CrossRef](#)]
24. Porwal, P.; Pachade, S.; Kamble, R.; Kokare, M.; Deshmukh, G.; Sahasrabudhe, V.; Meriaudeau, F. Indian diabetic retinopathy image dataset (IDRiD): A database for diabetic retinopathy screening research. *Data* **2018**, *3*, 25. [[CrossRef](#)]
25. Decencière, E.; Zhang, X.; Cazuguel, G.; Lay, B.; Cochener, B.; Trone, C.; Gain, P.; Ordóñez-Varela, J.-R.; Massin, P.; Erginay, A.; et al. Feedback on a publicly distributed image database: The Messidor database. *Image Anal. Stereol.* **2014**, *33*, 231–234. [[CrossRef](#)]
26. Niemeijer, M.; Staal, J.J.; Ginneken, B.; Loog, M.; Abramoff, M.D. DRIVE: Digital retinal images for vessel extraction. Methods for evaluating segmentation and indexing techniques dedicated to retinal ophthalmology. *IEEE Trans. Med. Imaging* **2004**, *23*, 501–509.
27. Goldbaum, M.D.M.; Hoover, A. *STARE Dataset Website*; Clemson University: Clemson, SC, USA, 1975.
28. Wang, H.; Yuan, G.; Zhao, X.; Peng, L.; Wang, Z.; He, Y.; Yingchuan, F.; Peng, Z. Hard exudate detection based on deep model learned information and multi-feature joint representation for diabetic retinopathy screening. *Comput. Methods Programs Biomed.* **2020**, *191*, 105398. [[CrossRef](#)]
29. Orlando, J.I.; Prokofyeva, E.; Del Fresno, M.; Blaschko, M.B. An ensemble deep learning based approach for red lesion detection in fundus images. *Comput. Methods Programs Biomed.* **2018**, *153*, 115–127. [[CrossRef](#)]
30. Zago, G.T.; Andreão, R.V.; Dorizzi, B.; Salles, E.O.T. Diabetic retinopathy detection using red lesion localization and convolutional neural networks. *Comput. Biol. Med.* **2020**, *116*, 103537. [[CrossRef](#)] [[PubMed](#)]
31. Atli, I.; Gedik, O.S. Sine-Net: A fully convolutional deep learning architecture for retinal blood vessel segmentation. *Eng. Sci. Technol. Int. J.* **2021**, *24*, 271–283. [[CrossRef](#)]
32. Badgujar, R.D.; Deore, P.J. Hybrid nature inspired SMO-GBM classifier for exudate classification on fundus retinal images. *IRBM* **2019**, *40*, 69–77. [[CrossRef](#)]
33. Yadav, D.; Karn, A.K.; Giddalur, A.; Dhiman, A.; Sharma, S.; Yadav, A.K. Microaneurysm detection using color locus detection method. *Measurement* **2021**, *176*, 109084. [[CrossRef](#)]
34. Imani, E.; Pourreza, H.R. A novel method for retinal exudate segmentation using signal separation algorithm. *Comput. Methods Programs Biomed.* **2016**, *133*, 195–205. [[CrossRef](#)]
35. Amin, J.; Sharif, M.; Yasmin, M.; Ali, H.; Fernandes, S.L. A method for the detection and classification of diabetic retinopathy using structural predictors of bright lesions. *J. Comput. Sci.* **2017**, *19*, 153–164. [[CrossRef](#)]
36. Mahendran, G.; Dhanasekaran, R. Investigation of the severity level of diabetic retinopathy using supervised classifier algorithms. *Comput. Electr. Eng.* **2015**, *45*, 312–323. [[CrossRef](#)]

37. Kumar, S.; Adarsh, A.; Kumar, B.; Singh, A.K. An automated early diabetic retinopathy detection through improved blood vessel and optic disc segmentation. *Opt. Laser Technol.* **2020**, *121*, 105815. [[CrossRef](#)]
38. Adem, K. Exudate detection for diabetic retinopathy with circular Hough transformation and convolutional neural networks. *Expert Syst. Appl.* **2018**, *114*, 289–295. [[CrossRef](#)]
39. Adal, K.M.; Sidibé, D.; Ali, S.; Chaum, E.; Karnowski, T.P.; Mériaudeau, F. Automated detection of microaneurysms using scale-adapted blob analysis and semi-supervised learning. *Comput. Methods Programs Biomed.* **2014**, *114*, 1–10. [[CrossRef](#)]
40. Garifullin, A.; Lensu, L.; Uusitalo, H. Deep Bayesian baseline for segmenting diabetic retinopathy lesions: Advances and challenges. *Comput. Biol. Med.* **2021**, *136*, 104725. [[CrossRef](#)] [[PubMed](#)]
41. Xia, H.; Lan, Y.; Song, S.; Li, H. A multi-scale segmentation-to-classification network for tiny microaneurysm detection in fundus images. *Knowl.-Based Syst.* **2021**, *226*, 107140. [[CrossRef](#)]
42. He, W.; Wang, X.; Wang, L.; Huang, Y.; Yang, Z.; Yao, X.; Zhao, X.; Ju, L.; Wu, L.; Lu, H.; et al. Incremental learning for exudate and hemorrhage segmentation on fundus images. *Inf. Fusion* **2021**, *73*, 157–164. [[CrossRef](#)]
43. Liu, Q.; Zou, B.; Chen, J.; Ke, W.; Yue, K.; Chen, Z.; Zhao, G. A location-to-segmentation strategy for automatic exudate segmentation in colour retinal fundus images. *Comput. Med. Imaging Graph.* **2017**, *55*, 78–86. [[CrossRef](#)] [[PubMed](#)]
44. Du, J.; Zou, B.; Chen, C.; Xu, Z.; Liu, Q. Automatic microaneurysm detection in fundus image based on local cross-section transformation and multi-feature fusion. *Comput. Methods Programs Biomed.* **2020**, *196*, 105687. [[CrossRef](#)]
45. Cao, P.; Ren, F.; Wan, C.; Yang, J.; Zaiane, O. Efficient multi-kernel multi-instance learning using weakly supervised and imbalanced data for diabetic retinopathy diagnosis. *Comput. Med. Imaging Graph.* **2018**, *69*, 112–124. [[CrossRef](#)]
46. Fraz, M.M.; Jahangir, W.; Zahid, S.; Hamayun, M.M.; Barman, S.A. Multi-scale segmentation of exudates in retinal images using contextual cues and ensemble classification. *Biomed. Signal Process. Control* **2017**, *35*, 50–62. [[CrossRef](#)]
47. Zhang, W.; Zhong, J.; Yang, S.; Gao, Z.; Hu, J.; Chen, Y.; Yi, Z. Automated identification and grading system of diabetic retinopathy using deep neural networks. *Knowl.-Based Syst.* **2019**, *175*, 12–25. [[CrossRef](#)]
48. Liao, Y.; Xia, H.; Song, S.; Li, H. Microaneurysm detection in fundus images based on a novel end-to-end convolutional neural network. *Biocybern. Biomed. Eng.* **2021**, *41*, 589–604. [[CrossRef](#)]
49. Sandhya, S.G.; Suhasini, A. An efficient detection of micro aneurysms from fundus images with CDLNN algorithm. *Mater. Today Proc.* **2021**. [[CrossRef](#)]
50. Sambyal, N.; Saini, P.; Syal, R.; Gupta, V. Modified U-Net architecture for semantic segmentation of diabetic retinopathy images. *Biocybern. Biomed. Eng.* **2020**, *40*, 1094–1109. [[CrossRef](#)]
51. Sugeno, A.; Ishikawa, Y.; Ohshima, T.; Muramatsu, R. Simple methods for the lesion detection and severity grading of diabetic retinopathy by image processing and transfer learning. *Comput. Biol. Med.* **2021**, *137*, 104795. [[CrossRef](#)] [[PubMed](#)]
52. Khojasteh, P.; Júnior, L.A.P.; Carvalho, T.; Rezende, E.; Aliahmad, B.; Papa, J.P.; Kumar, D.K. Exudate detection in fundus images using deeply-learnable features. *Comput. Biol. Med.* **2019**, *104*, 62–69. [[CrossRef](#)] [[PubMed](#)]
53. Gayathri, S.; Gopi, V.P.; Palanisamy, P. A lightweight CNN for Diabetic Retinopathy classification from fundus images. *Biomed. Signal Process. Control* **2020**, *62*, 102115.
54. Deepa, V.; Kumar, C.S.; Cherian, T. Ensemble of multi-stage deep convolutional neural networks for automated grading of diabetic retinopathy using image patches. *J. King Saud Univ. Comput. Inf. Sci.* **2022**, *34*, 6255–6265. [[CrossRef](#)]